Institut für Physik
Arbeitsgruppe “Nichtlineare Dynamik”

Feedback Control of Complex Oscillatory Systems

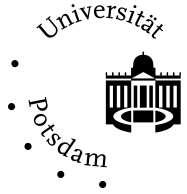

Dissertation
zur Erlangung des akademischen Grades
“doctor rerum naturalium”
(Dr. rer. nat.)
in der Wissenschaftsdisziplin “Theoretische Physik”

eingereicht an der
Mathematisch-Naturwissenschaftlichen Fakultät
der Universität Potsdam

von
Natalia Tukhlina

Potsdam, Februar 2008

This work is licensed under a Creative Commons License:
Attribution - Noncommercial - Share Alike 3.0 Unported
To view a copy of this license visit
http://creativecommons.org/licenses/by-nc-sa/3.0/

Online published at the
Publikationsserver der Universität Potsdam:
http://opus.kobv.de/ubp/volltexte/2008/1854/
urn:nbn:de:kobv:517-opus-18546
[http://nbn-resolving.de/urn:nbn:de:kobv:517-opus-18546]

Contents

Abstract

In the present dissertation paper an approach which ensures an efficient control of such diverse systems as noisy or chaotic oscillators and neural ensembles is developed. This approach is implemented by a simple linear feedback loop. The dissertation paper consists of two main parts. One part of the work is dedicated to the application of the suggested technique to a population of neurons with a goal to suppress their synchronous collective dynamics. The other part is aimed at investigating linear feedback control of coherence of a noisy or chaotic self-sustained oscillator.

First we start with a problem of suppressing synchronization in a large population of interacting neurons. The importance of this task is based on the hypothesis that emergence of pathological brain activity in the case of Parkinson's disease and other neurological disorders is caused by synchrony of many thousands of neurons.

The established therapy for the patients with such disorders is a permanent high-frequency electrical stimulation via the depth microelectrodes, called Deep Brain Stimulation (DBS). In spite of efficiency of such stimulation, it has several side effects and mechanisms underlying DBS remain unclear. In the present work an efficient and simple control technique is suggested. It is designed to ensure suppression of synchrony in a neural ensemble by a minimized stimulation that vanishes as soon as the tremor is suppressed. This vanishing-stimulation technique would be a useful tool of experimental neuroscience; on the other hand, control of collective dynamics in a large population of units represents an interesting physical problem. The main idea of suggested approach is related to the classical problem of oscillation theory, namely the interaction between a self-sustained (active) oscillator and a passive load (resonator). It is known that

under certain conditions the passive oscillator can suppress the oscillations of an active one. In this thesis a much more complicated case of active medium, which itself consists of thousands of oscillators is considered. Coupling this medium to a specially designed passive oscillator, one can control the collective motion of the ensemble, specifically can enhance or suppress it. Having in mind a possible application in neuroscience, the problem of suppression is concentrated upon.

Second, the efficiency of suggested suppression scheme is illustrated by considering more complex case, i.e. when the population of neurons generating the undesired rhythm consists of two non-overlapping subpopulations: the first one is affected by the stimulation, while the collective activity is registered from the second one. Generally speaking, the second population can be by itself both active and passive; both cases are considered here. The possible applications of suggested technique are discussed.

Third, the influence of the external linear feedback on coherence of a noisy or chaotic self-sustained oscillator is considered. Coherence is one of the main properties of self-oscillating systems and plays a key role in the construction of clocks, electronic generators, lasers, etc. The coherence of a noisy limit cycle oscillator in the context of phase dynamics is evaluated by the phase diffusion constant, which is in its turn proportional to the width of the spectral peak of oscillations. Many chaotic oscillators can be described within the framework of phase dynamics, and, therefore, their coherence can be also quantified by the way of the phase diffusion constant. The analytical theory for a general linear feedback, considering noisy systems in the linear and Gaussian approximation is developed and validated by numerical results.

Zusammenfassung

In der vorliegenden Dissertation wird eine Näherung entwickelt, die eine effiziente Kontrolle verschiedener Systeme wie verrauschten oder chaotischen Oszillatoren und Neuronenensembles ermöglicht. Diese Näherung wird durch eine einfache lineare Rückkopplungsschleife implementiert. Die Dissertation besteht aus zwei Teilen. Ein Teil der Arbeit ist der Anwendung der vorgeschlagenen Technik auf eine Population von Neuronen gewidmet, mit dem Ziel ihre synchrone Dynamik zu unterdrücken. Der zweite Teil ist auf die Untersuchung der linearen Feedback-Kontrolle der Kohärenz eines verrauschten oder chaotischen, selbst erregenden Oszillators gerichtet.

Zunächst widmen wir uns dem Problem, die Synchronisation in einer großen Population von aufeinander wirkenden Neuronen zu unterdrücken. Da angenommen wird, dass das Auftreten pathologischer Gehirntätigkeit, wie im Falle der Parkinsonschen Krankheit oder bei Epilepsie, auf die Synchronisation großer Neuronenpopulation zurück zu führen ist, ist das Verständnis dieser Prozesse von tragender Bedeutung. Die Standardtherapie bei derartigen Erkrankungen besteht in einer dauerhaften, hochfrequenten, intrakraniellen Hirnstimulation mittels implantierter Elektroden (Deep Brain Stimulation, DBS). Trotz der Wirksamkeit solcher Stimulationen können verschiedene Nebenwirkungen auftreten, und die Mechanismen, die der DBS zu Grunde liegen sind nicht klar. In meiner Arbeit schlage ich eine effiziente und einfache Kontrolltechnik vor, die die Synchronisation in einem Neuronenensemble durch eine minimierte Anregung unterdrückt und minimalinvasiv ist, da die Anregung stoppt, sobald der Tremor erfolgreich unterdrückt wurde. Diese Technik der "schwindenden Anregung" wäre ein nützliches Werkzeug der experimentellen Neurowissenschaft. Desweiteren stellt die Kontrolle der kollektiven Dynamik in einer großen Population von

Einheiten ein interessantes physikalisches Problem dar. Der Grundansatz der Näherung ist eng mit dem klassischen Problem der Schwingungstheorie verwandt - der Interaktion eines selbst erregenden (aktiven) Oszillators und einer passiven Last, dem Resonator. Ich betrachte den deutlich komplexeren Fall eines aktiven Mediums, welches aus vielen tausenden Oszillatoren besteht. Durch Kopplung dieses Mediums an einen speziell hierür konzipierten, passiven Oszillator kann man die kollektive Bewegung des Ensembles kontrollieren, um diese zu erhöhen oder zu unterdrücken. Mit Hinblick auf eine möglichen Anwendung im Bereich der Neurowissenschaften, konzentriere ich mich hierbei auf das Problem der Unterdrückung.

Im zweiten Teil wird die Wirksamkeit dieses Unterdrückungsschemas im Rahmen eines komplexeren Falles, bei dem die Population von Neuronen, die einen unerwünschten Rhythmus erzeugen, aus zwei nicht überlappenden Subpopulationen besteht, dargestellt. Zunächst wird eine der beiden Subpopulationen durch Stimulation beeinflusst und die kollektive Aktivität an der zweiten Subpopulation gemessen. Im Allgemeinen kann sich die zweite Subpopulation sowohl aktiv als auch passiv verhalten. Beide Fälle werden eingehend betrachtet. Anschließend werden die möglichen Anwendungen der vorgeschlagenen Technik besprochen.

Danach werden verschiedene Betrachtungen über den Einfluss des externen linearen Feedbacks auf die Kohärenz eines verrauschten oder chaotischen selbst erregenden Oszillators angestellt. Kohärenz ist eine Grundeigenschaft schwingender Systeme und spielt ein tragende Rolle bei der Konstruktion von Uhren, Generatoren oder Lasern. Die Kohärenz eines verrauschten Grenzzyklus Oszillators im Sinne der Phasendynamik wird durch die Phasendiffusionskonstante bewertet, die ihrerseits zur Breite der spektralen Spitze von Schwingungen proportional ist. Viele chaotische Oszillatoren können im Rahmen der Phasendynamik beschrieben werden, weshalb ihre Kohärenz auch über die Phasendiffusionskonstante gemessen werden kann. Die analytische Theorie eines allgemeinen linearen Feedbacks in der Gauß'schen, als auch in der linearen, Näherung wird entwickelt und durch numerische Ergebnisse gestützt.

Chapter 1

Introduction

Feedback control is a basic mechanism by which many systems, whether mechanical, electrical, or biological, maintain their equilibrium or other desired dynamical behavior. Control systems of various types date back to antiquity, all the way to the need for accurate determination of time in Greek and Arab water clocks. The first water clocks represented a tank holding water with a very small hole in its bottom, from which the water slowly drips. The level of water sinks and its height is a measure of the time passed since it was full of water. Remarkably, that the expression "much water has flowed under the bridge since then" probably came from the water clocks. In the 3rd century B.C., Ctesibius or Ktesibios of Alexandria, Egypt, a Greek physicist and inventor, improved the construction of the water clocks by adding a float regulator. The function of this regulator was to keep the water level in a tank at a constant depth. This constant depth yielded a constant flow of water through a tube at the bottom of the tank which filled a second tank at a constant rate. The level of water in the second tank was thus proportional to the time elapsed.

The pivotal moment in the development of the control engineering was the invention of the steam engine governor by J. Watt in 1769 — an essential contribution to the Industrial Revolution. The classical control theory arose from a requirement to implement and analyze a stable performance of the engine governor and other technological systems. The basis of the theory was laid by the famous J.C. Maxwell (1) in 1868 and independently by the Russian scientist I.A. Vyshnegradskii (2) in 1876. In their works, they modelled the dynamics of a steam

engine with a Watt's governor and performed the corresponding mathematical analysis. In particular, their studies explained instability and onset of hunting. Since then, the development of the control theory was tightly interrelated with the development of nonlinear physics, i.e., with the theory of oscillations and nonlinear dynamics. However, in the works of Maxwell and Vyshnegradskii the stability analysis of the governor was done under assumption that Coulomb friction of the governor coupling (clutch) can be neglected, so that the differential equations of motion are linearized. Taking into account the nonlinearities, such as the Coulomb friction in the control loop, makes the analysis much more complicated. This full nonlinear problem remained unsolved for many years.

The decisive step in the development of nonlinear science was stimulated by rapid strides in electrical and radio engineering in the 1920's. The pioneering work regarding the propagation of radio waves and nonlinear oscillations has been done by van der Pol (3) and Appleton (4). The next essential impact on this field, in particular on the development of mathematical tools for solving nonlinear problems, has been given by A.A. Andronov and his school. Together with A.G. Maier he succeeded in resolving the problem, first considered by Maxwell and Vyshnegradskii. Andronov and Maier made a great advance taking into account the effect of Coulomb friction on a system and thus considering a nonlinear three-dimensional system of differential equations (5; 6). This nonlinear problem was solved by virtue of a mapping technique, developed by Andronov and Maier (7). This method is a generalization of Andronov's own work on limit cycles, which was extended to higher dimensions of the state space and was used by Andronov to address a number of other nonlinear problems in automatic control.

In the subsequent years, feedback control has been used in many areas of engineering and technology. It is worth singling out two main trends and key inventions namely, mass communications and the aerospace industry. The main problem in the development of long-distance communication was to increase the signal-to-noise ratio of an amplifier so that it amplifies only the voice signal, but not the noise. For this purpose the electrical engineer H. S. Black used a negative feedback loop (8). An important contribution to the aerospace industry was done by R. Kalman, who developed an efficient recursive filter that provides accurate continuously-updated information about the internal state of a dynamical system

from a set and noisy measurements (9). The Kalman filter is essentially a set of mathematical equations that provides an efficient computational method to estimate the location of the target at the present time (filtering), at a future time (prediction), or at a time in the past (interpolation or smoothing). It is used in a wide range of engineering applications from radar to computer vision. Another notable example for control in aerospace technologies comes from the control of flight, namely the problem of dynamics of an airplane supplied by the autopilot device, which has been investigated by Andronov and his student Bautin (10). A detailed historical review of control theory is given in (11).

Feedback control is useful not only for engineering aspects of experiments but also has found applications in various fields of physics (12) such as chaos and nonlinear dynamics, statistical mechanics and optics. Particularly, a delayed feedback is a commonly employed tool to control different properties of a dynamical system: to make chaotic systems operate periodically (famous Pyragas' control method (13)), to suppress space-time chaos (14; 15; 16; 17), to manipulate coherence of noisy periodic and chaotic oscillators (18; 19; 20). Feedback mechanisms are ubiquitous in science and nature. For example, global climate dynamics depend on the feedback interactions between the atmosphere, oceans, land, and the sun. Many other examples of feedback regulation can be found in living organisms; thus, feedback mechanisms play an important role in the regulation of respiratory and cardiac rhythms (21; 22).

Before formulating the problem of the present doctoral study, we discuss a physical problem that – at first glance – is not related to the field of feedback control. This problem considers an interaction of an active system (or medium) with a passive one. So, classical oscillation theory treats interaction between an active, self-sustained oscillator and a passive load resonator. It is known (see, e.g., (23)), that there is a certain parameter range when the passive system can quench the active one. In a more complex formulation, one can analyze the dynamics of an ensemble of (infinitely) many interacting units for the case when some units are in the regime of self-sustained oscillations whereas the other units are passive. Thus, one can speak of interaction between active and passive subpopulations. The dynamics of such mixed populations of oscillators has been investigated in (24; 25). It was reported that the collective dynamics of the

ensemble (mean field) depends on the ratio between the numbers of active and passive oscillators. In particular, for certain ratios and parameters the mean field oscillation vanishes.

The main idea of the present doctoral study is to use the physical problem (interaction of an active and a passive medium) described above, for the purpose of control of complex systems. This link of nonlinear dynamics and control theory provides efficient and easily implemented algorithms. Namely, we exploit specialy designed passive systems in order to control such diverse complex dynamical systems as a neural population and a noisy or chaotic self-sustained oscillatory system. In the language of control theory it means that we design a special feedback loop.

In particular, we consider two problems. The first problem addressed in this thesis is related to the role of a macroscopic rhythmical neural activity in a pathological brain functioning. Namely, it is related to the hypothesis that some neurological diseases, in particular Parkinson's disease and essential tremor are associated with an abnormal synchronization of many oscillators (26; 27; 28)). Correspondingly, suppression of this pathological synchronous activity or, in other words, *desynchronization* of a neuronal ensemble is a crucial problem of neuroscience. The standard therapy, which is used nowadays for treatment of intractable Parkinsonian tremor is electrical Deep Brain Stimulation (DBS) (29; 30; 31). This surgical technique involves implanting a microelectrode into subcortical structure in the brain for high frequency (greater then 100 Hz) long-term stimulation. When this procedure is successful, the abnormal tremor is abolished. Although results of this therapy are impressive, DBS has some limitations and several side effects. The high frequency Deep Brain Stimulation was developed empirically, based on surgical procedures and the mechanism by which this electrical stimulation suppresses tremor is still unknown. Thus, the development of more mild and effective technique for suppression of undesired synchronous dynamics of neural population constitutes a significant problem. A number of methods have been suggested recently and they can be roughly classified into two approaches: non-feedback (see (26; 32) and references therein) and feedback techniques ((33; 34; 35; 36)). A simple and effective technique, which enables the restoration of desynchronized dynamics in a network of oscillatory

neurons is developed and presented in the current work (37). This technique is based on the design of a passive unit coupled to the neuronal population to be controlled. From the control theory viewpoint, it means designing of a linear feedback loop with a built-in second-order filter.

The destruction of undesirable synchronous oscillation is accomplished in the following way. The activity of a neural population is permanently measured and fed back after linear prossesing. The main advantage of the suggested technique, is that the administered control input vanishes as soon as desynchronized state is achieved. This feature is significant for therapeutic applications, since it means reduction of intervention into a living tissue. Further, the efficiency of the suggested suppression scheme is illustrated by considering more complex case, i.e. when the population of neurons generating the undesired rhythm consists of two non-overlapping subpopulations: first one is affected by the stimulation, and the collective activity is measured from the second one. Possible applications of the suggested technique are discussed.

The second problem, which is studied in the present thesis is control of a noisy self-oscillatory or chaotic system. In particular, our goal is to control one of the crucial characteristic of the dynamics of such systems, which is coherence, or constancy of frequency. The coherence of a noisy limit cycle oscillator in the context of phase dynamics is evaluated by the phase diffusion constant, which is in its turn proportional to the width of the spectral peak of oscillations. Many chaotic oscillators can be described within the framework of phase dynamics, and, therefore, their coherence can be also quantified by the way of a phase diffusion constant. Coherence plays a key role in the construction of clocks, electronic generators, lasers, etc. In this thesis it is demonstrated that coherence of a noisy or chaotic self-sustained oscillator can be efficiently manipulated by a *linear feedback*. It should be stressed that the goal is not to suppress chaos, but to control the diffusion constant. An analytical theory for a general linear feedback, considering noisy systems in the linear and Gaussian approximation is developed and proved by numerical results.

The present thesis has the following structure. Chapter 2 is devoted to the problem of suppression of neuronal synchrony; here the proposed feedback scheme is described and analyzed. The efficiency of the control technique is illustrated

by an example of an isolated neuronal ensemble. Further, the same topic is addressed, but in a more complex formulation, when the population of neurons consists of two interacting subpopulations, one active and one passive. In Chapter 3 we turn our attention to the problem of utilizing general linear feedback to control coherence of noisy or chaotic self-oscillatory systems. Chapter 4 presents conclusions and discussion.

Chapter 2

Feedback suppression of neural synchrony by vanishing stimulation

Collective dynamics of large population of neurons is widely studied in neurophysiological experiments as well as in theoretical works. These studies are motivated by the importance of macroscopic rhythmical neural activity in physiological and pathological brain functioning (see, e.g., (26; 27; 28) and references therein). On the other hand, the understanding of cooperative behavior in a large ensemble of interacting units constitutes an essential problem of nonlinear dynamics. In particular, the problem of high practical importance is to develop techniques for *control* of collective neuronal activity. The significance of this task is motivated by the hypothesis that pathological brain rhythms, which are registered by means of electro- or magnetoencephalography in patients suffering from Parkinson's disease and essential tremor syndrome, appear due to synchrony in many thousands of neurons. Obviously, quenching of these rhythms constitutes a challenging problem of neuroscience and a number of techniques has been proposed in order to solve this problem. All these approaches are aimed to improve the technique, currently used in medical practice and known as *Deep Brain Stimulation(DBS)*.

2.1 Controlling neural synchrony

2.1.1 Electrical stimulation of brain structures

For a couple of decades the electrical stimulation of the human brain has been used in pilot studies with the aim of suppressing the pathological activity in epilepsy (29; 30) and, with more successful clinical applications, in Parkinsons disease (31). This surgical procedure, called Deep Brain Stimulation (DBS), implies *permanent* electrical stimulation of certain brain structures via implanted microelectrodes. In Parkinsonian patients, DBS at frequencies greater than 100 Hz has been shown to relieve tremor as well as other symptoms such as rigidity and dyskinesia. It decreases tremor amplitude in a spectacular way; the illustration of this effect with real data can be found on the PhysioNet web page [1]. Noteworthy, in spite of rather broad usage of DBS the neurophysiological mechanisms of such stimulation are poorly (if at all) understood. To our knowledge, the only analysis of the action of high-frequency stimulation with the help of a realistic model of the brain circuitry involved in the tremor generation has been undertaken in Ref. (38). Although, effects of DBS are impressive, DBS has been developed empirically and has some significant drawbacks and limitations. Namely, the parameters of the stimulation must be determined by trial and error and re-adjusted with time. Next, a certain amount of patients do not respond to DBS (39); some patients may become tolerant of stimulation in time, thus, the stimulation has to be increased over the years, in order to maintain the tremor suppressive effect. Moreover, the energy consumption of the permanent stimulation is quite high. Thus, the battery in the controller has to be exchanged after 1-3 years by means of a surgery. Finally, permanent stimulation definitely represents a very strong intervention into the system. Correspondingly, there is a significant clinical need for mild and effective suppression technique, which would provide destruction of a pathological brain activity by a minimized stimulation.

[1] URL: www.physionet.org/physiobank/database/tremordb/

2.1.2 Development of model-based stimulation techniques

Several methods for a suppression of neural synchrony, closely related to the theoretical understanding of the problem, have been suggested recently. The ultimate goal of these theoretical studies is to substitute the DBS by a more intelligent stimulation technique. One theoretical approach to desynchronization is based on the implementation of phase resetting of ensemble elements by precisely timed pulses (see (26; 32) and references therein), whereas another approach exploits a time-delayed feedback (34; 35; 33; 36). Although motivated by applications in neuroscience, both methods are of general interest, because a control of collective dynamics in a large population of units is not only relevant because of possible neuroscience applications, but represents an interesting physical problem. The mostly illustrative example of a physical system, where collective synchrony was highly undesirable and had to be suppressed, is the London Millennium bridge that exhibited high-amplitude lateral sway on the day of its opening (40; 41). We mention here also recent experiments on desynchronization of a population of coupled electrochemical oscillators (42).

2.1.3 Synchrony in neural populations

A commonly used theoretical description of macroscopical brain rhythms assumes their appearance due to synchronization in a large population of interacting neurons (26), when a large part or all units adjust their rhythms and produce a non-zero mean field, which has the same frequency as the synchronized majority. This viewpoint is supported by experimental observations (43; 44; 45; 46). Because of a rich connectivity in such a population, the dynamics is often modelled by an ensemble of dynamical neurons with an all-to-all coupling. The simplest model for the synchronization in such an ensemble is a Kuramoto transition (47; 48) in a population of all-to-all coupled phase oscillators: if the coupling strength ε in the ensemble exceeds some threshold value ε_{cr}, the macroscopic mean field appears and its amplitude growth with the super-criticality $\varepsilon - \varepsilon_{cr}$. This transition is often considered in an analogy to second order phase transitions; on the other hand, it can be viewed at as a supercritical Hopf bifurcation for the mean field. Correspondingly, the problem of suppression of neural synchrony is often formulated

as the problem of *desynchronization of a large neuronal population* (26). This means that the desired stimulation technique should not suppress oscillations of individual neurons, but only destroy the synchrony between them. Another important requirement is to minimize the intervention into the live system by reducing the intensity of the applied stimulation.

Although analytical treatment of Kuramoto-like models is possible only for fully connected ensembles (what is certainly not true in real systems), this approximation is considered to be reasonable, due to a relatively high connectivity in neuronal networks.We illustrate the Kuramoto transition by an example, considering an ensemble of N Bonhoeffer - van der Pol oscillators (with $N \to \infty$ in the thermodynamic limit), coupled via the mean field in the x variable:

$$\begin{aligned} \dot{x}_i &= x_i - x_i^3/3 - y_i + I_i + \varepsilon X \ , \\ \dot{y}_i &= 0.1(x_i + 0.7 - 0.8y_i) \ . \end{aligned} \tag{2.1}$$

Each unit is driven by the force εX, where ε quantifies the strength of the mean field coupling and $X = N^{-1}\sum_{i=1}^{N} x_i$ is the mean field. Parameter I_i has the meaning of the external current and directly influences the spiking frequency of elements of the ensemble. The elements are not identical: parameter I_i is taken as $I_i = 0.6 + \sigma$, where σ is a Gaussian distributed number with zero mean and 0.1 rms value. For the coupling strength below the critical value, $\varepsilon < \varepsilon_{cr} \approx 0.015$, one observes small irregular fluctuations of the mean field X around $X_0 \approx -0.25$ (see the red line in Fig. 2.1(a) for an example computed for $N = 500$ and $\varepsilon = 0.01$); these fluctuations are due to the finite size of the ensemble. With the increase of ε beyond the critical value $\varepsilon > \varepsilon_{cr} \approx 0.015$, the oscillators of the ensemble synchronize (see the black line in Fig. 2.1(a) computed for $\varepsilon = 0.03$).

2.1.4 Suggested approach

In this chapter we develop and analyze an efficient technique for desynchronization in a population of interacting units. The main requirement for this method is to provide a *vanishing-stimulation control*[2]. That is, the magnitude of the control input (stimulation) $\mathcal{C}$ should be proportional to the synchronous rhythmic

[2]In the context of chaos control the schemes with vanishing feedback signal are sometimes called noninvasive. Having in mind possible applications in neuroscience, we prefer not to use

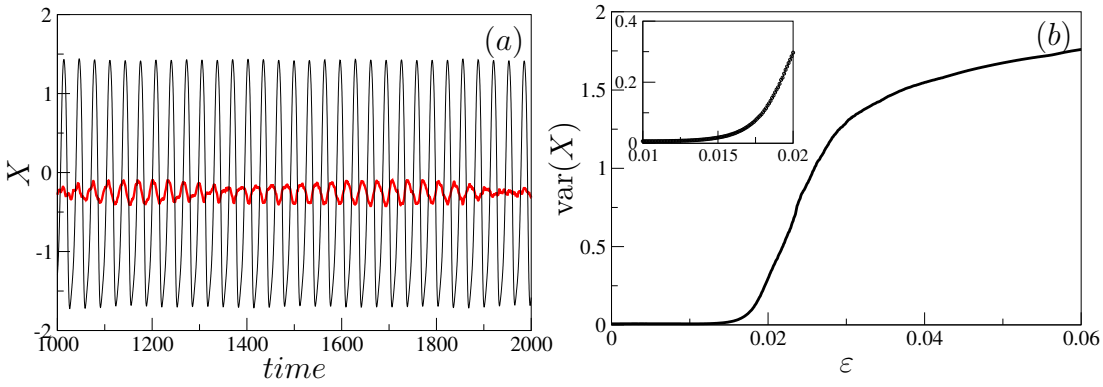

Figure 2.1: (a) The evolution of the mean field in the population of 500 Bonhoeffer – van der Pol neurons (Eqs. (2.1)) for subcritical coupling $\varepsilon = 0.01$ (red line) and supercritical coupling $\varepsilon = 0.03$ (black line). (b) Transition to the macroscopic mean field in the model (2.1).

activity and must vanish as soon as the suppression is achieved. This can be accomplished by a feedback technique, where the control input decreases to the fluctuation level as soon as the rhythm is suppressed. Accordingly, we assume that in an experiment the mean field (or a related quantity, see Section 2.3.2) can be measured and subsequently used for stimulation of the ensemble via a feedback loop (see Fig. 2.2 below).

From a rather general physical viewpoint the population of neural oscillators to be controlled can be considered as an active medium. The main idea of our approach is to couple it to an *additional passive oscillator*. If we model the dynamics of the active medium by a single non-zero mode, then the problem is similar to a classical problem of the oscillation theory and nonlinear dynamics, where an interaction of an active, self-sustained oscillator, with a passive load (resonator) has been considered (see, e.g., (23)). It is known, that under certain condition such a passive system can quench the active oscillator. Similarly, the appearance of collective synchronization in a mixed population of active and passive oscillators depends on the proportion of passive elements; this effect, called aging, has attracted attention recently (for instance see (24; 25)). However, in the context of neuroscience applications, a special consideration is necessary, because

this term here, because in this field any measurement/stimulation using implanted electrodes is considered as invasive.

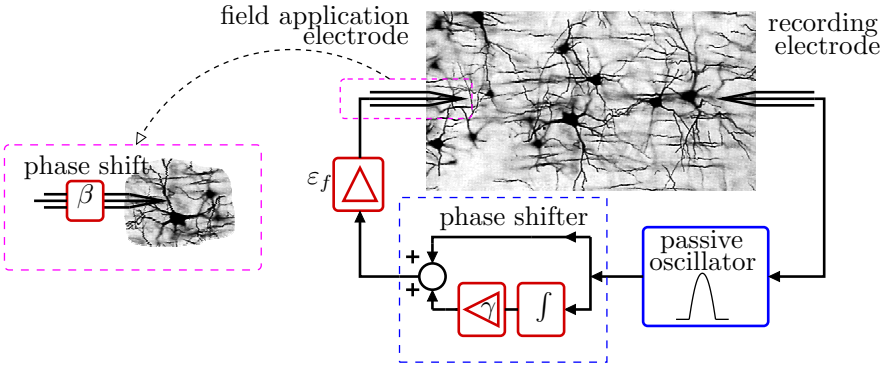

Figure 2.2: Suggested suppression scheme. The local field potential related to the mean field of the population is measured by the recording electrode and is fed back via the field application electrode. The feedback loop contains a passive oscillator playing the role of a band pass filter, an integrator, a summator, and two amplifiers. Stimulation is characterized by an *a priori* unknown phase shift.

there appear three additional requirements to the suppression scheme: (i) the stimulation should compensate the unknown phase shift inherent to stimulation (see Fig. 2.2 and discussion below); (ii) the controller should be able to extract the relevant signal from its mixture with the rhythms produced by neighbouring neuronal populations and with the measuremental noise; (iii) the control scheme should be able to compensate the *latency* in measurements. In our approach, presented below, we construct an auxiliary passive oscillator whose interaction with the ensemble of all-to-all coupled active units destroys the collective synchrony under the requirements formulated.

2.2 Stabilization of an active oscillator by a passive one

Suppression of an undesired rhythm can be considered as a stabilization of an unknown unstable steady state of a complex multi-dimensional system. Stabilization of steady states is a classical problem of the control theory. A common approach to treat this problem is to implement a feedback control. Typically, the feedback signal is proportional to the deviation of a coordinate of the sys-

tems from the desired state (proportional control), or to the derivative of the coordinate (proportional-derivative control), or to the integral of the coordinate over the past (proportional-integral control), or to a combination of these three values (12). Another group of stabilization techniques uses linear or nonlinear *time-delayed* feedback, see, e.g., (13; 49; 50; 51; 52; 53). For low-dimensional systems (see, e.g., (54; 55) and references therein), the theory of feedback stabilization is well-developed and finds many technical applications. In this Section we consider the stabilization problem on a macroscopic level, taking into account only the collective motion. In this way the problem is reduced to stabilization of a low-dimensional dynamics. However, the known techniques generally do not meet the above formulated requirements and therefore are not appropriate for the considered neuroscience application. Thus, we assume that the collective oscillating mode is active and close to a Hopf bifurcation:

$$\dot{A} = (\xi + i\omega)A - |A|^2 A + \mathcal{C}e^{i\beta} \, . \tag{2.2}$$

Here A is the complex amplitude of oscillations having frequency ω, ξ is the dimensionless parameter describing the instability of the equilibrium $A = 0$, which we want to stabilize, and $\mathcal{C}$ is the control signal (stimulation). The parameter β describes the uncertainty of our action on the active oscillator: in a realistic application, the way the external force is coming in the equations is typically unknown.

Our aim is to construct the control signal $\mathcal{C}$ based on a scalar observable which, without lost of generality, can be chosen proportional to $X(t) = \text{const} + \text{Re}(A)$; here the constant reflects the fact that for neuronal models, the fixed point of collective oscillations is typically not at zero. (Note also that the case of other linear in A observable corresponds to a shift of the parameter β.) In (34; 35) a time-delayed proportional feedback $\mathcal{C}\sim(X(t-\tau) - X(t))$ has been suggested and treated numerically and analytically. Theory and simulation with bursting and spiking neurons, also with synaptic connections (36), as well as recent experiment (42), show that such a control scheme provides a reliable suppression of oscillations, i.e. $\text{var}(X) \to 0$, with vanishing stimulation, $\mathcal{C} \to 0$. On the contrary, if a feedback is proportional to the delayed mean field, $\mathcal{C} \sim X(t-\tau)$ (34; 35) or to its power (51; 52; 33), then the stimulation is generally not vanishing; i.e.

a permanent stimulation with $\mathcal{C} = \text{const}$ is required for the maintenance of the suppressed state, $\text{var}(X) \to 0$. A general disadvantage of a delayed feedback is a new, undesirable, instability, which the delay term can bring into the system. To overcome this, we suggest a suppression scheme without delay which exploits an additional passive oscillator.

The above formulated requirements for the suppression can be now specified as follows: (i) a constant component in the observed field should be washed out; (ii) there should be a possibility to vary the phase shift in the feedback loop in a large range, to be able to compensate for the unknown phase factor β and for a possible latency in the observations; (iii) noise and other components in the observed field which are not related to the main rhythm should be washed out.

Let us include in the control loop a linear damped oscillator in a way that it is driven by the measured signal:

$$\ddot{u} + \alpha\dot{u} + \omega_0^2 u = X(t) \; . \tag{2.3}$$

The parameter ω_0 is taken to be equal to the frequency ω of macroscopic oscillations in (2.2) without control; this frequency can be easily measured in an experiment. This means that the driven oscillator (2.3) is in resonance with the forcing (for a moment we can consider it as a harmonic one with the frequency ω) and the phase of the output u is shifted by $\pi/2$ with respect to the the phase of the input $X(t)$, whereas the phase shift of the derivative of the output signal $\dot{u}$ with respect to the input $X(t)$ is zero. It is important to note that the variable $\dot{u}$ does not contain a constant component, $\langle\dot{u}\rangle = 0$, even if the observed field does. Thus, stimulation proportional to $\dot{u}$ vanishes as soon as the control is successful, and the requirement (i) to the control strategy is fulfilled. Moreover, the output $\dot{u}$ can be considered as an application of a band pass filter to the input signal X, which filters out noise and other components outside of the vicinity of the main oscillation mode – this accomplishes the requirement (iii).

To compensate the unknown phase shift β (requirement (ii)) we include a unit described by the following equation:

$$\mu\dot{d} + d = \dot{u} \; . \tag{2.4}$$

For $\mu\omega \gg 1$ this unit operates as an integrator (with an additional multiplication by the factor $1/\mu$), whereas for $\omega \to 0$ its transfer function is 1. Hence, the output

of system (2.4) has the same average as the input, i.e. $\langle d \rangle = 0$. Finally, the control signal $\mathcal{C}$ is taken proportional to the weighted sum of $\dot{u}$ and d: $\mathcal{C} \sim \varepsilon_f(\dot{u} + \gamma d)$, where the parameter γ determines the desired phase shift. The units performing this summation and the integration according to Eq. (2.4) form the *phase shifter*. It is seen from Fig. 2.3 that the phase difference θ between the output $\dot{u} + \gamma d$ of the phase shifter and its input $\dot{u}$ is

$$\theta = -\arctan\left(\frac{\gamma}{\omega\mu}\right) , \tag{2.5}$$

and therefore can be arbitrary varied in the interval $-\pi/2 < \theta < \pi/2$. The

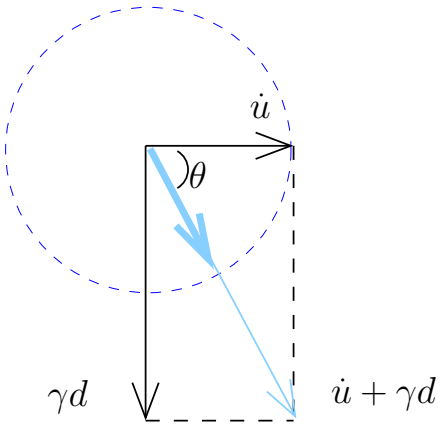

Figure 2.3: Illustration of the function of the phase shifter. The input to the shifter is represented by the vector $\dot{u}$. Integrator delays this input by $\pi/2$ and multiplies by $1/(\mu\omega)$, result of this operation is represented by vector d. The output of the shifter is the sum $\dot{u} + \gamma d$. It is easy to see that the phase difference θ between the output of the phase shifter and its input is determined by the free parameter γ according to Eq. (2.5). For the stimulation we use the output (bold blue line), normalized by $\sqrt{1 + \gamma^2/\omega^2\mu^2}$ (see Eq. (2.6)), what provides an independence of the amplification in the feedback loop from θ.

phase shift in the interval $\pi/2 < \theta < 3\pi/2$ can be obtained by the sign inversion: $\varepsilon_f \to -\varepsilon_f$. Summarizing, the control input $\mathcal{C}$ to the system is constructed as

$$\mathcal{C} = \pm\frac{\varepsilon_f}{\sqrt{1 + \gamma^2/\omega^2\mu^2}}(\dot{u} + \gamma d) = \varepsilon_f \cos\theta \cdot (\dot{u} - \omega\mu d \tan\theta) , \tag{2.6}$$

where $\sqrt{1 + \gamma^2/\omega^2\mu^2} = 1/\cos\theta$ is the normalization coefficient. It ensures an independence of the amplification in the feedback loop from the phase shift θ, so

that this amplification is completely determined by ε_f. At the points $\theta = \pm\pi/2$ the control term is calculated as $\mathcal{C} = \varepsilon_f \omega\mu d$.

To complete the design of the control loop, we have to choose the parameter α which is the damping factor of the oscillator (2.3). This parameter determines the width of the band pass, $\Delta f = \alpha/2\pi$. Having in mind the application to Parkinsonian rhythms with realistic values for the band pass from 10 to 13 Hz, we choose $\Delta f/f \approx 0.3$ what gives $\alpha = 0.3\omega$.

The final equations for the controlled system read

$$\begin{aligned} \dot{A} &= (\xi + i\omega)A - |A|^2 A + \frac{\varepsilon_f}{\sqrt{1+\gamma^2/\mu^2\omega^2}}(\dot{u} + \gamma d)e^{i\beta} , \\ \ddot{u} &+ \alpha\dot{u} + \omega^2 u = Re(A) , \\ \mu\dot{d} &+ d = \dot{u} . \end{aligned} \tag{2.7}$$

In the following we denote $\mathcal{E} = \varepsilon_f/\sqrt{1+\gamma^2/\mu^2\omega^2} = \varepsilon_f \cos\theta$.

The desired asynchronous state of the ensemble corresponds to the fixed point $A = 0$ in the model equation. To analyze the stability of this solution, we consider only the linear terms of Eqs. (2.7), substitute $A = x + iy$ and $\dot{u} = v$, and rewrite the system Eqs. (2.7) as a system of 5 real differential equations of first order. Seeking the solution in the form $x = Xe^{\lambda t}$, $y = Ye^{\lambda t}$, $u = Ue^{\lambda t}$, $v = Ve^{\lambda t}$, $d = De^{\lambda t}$, we obtain the algebraic system of 5 linear equations. This system has a non-trivial solution if its determinant is equal to 0; this condition provides the equation $f(\lambda, \mathcal{E}, \gamma) = 0$ (its exact form is given by Eq. (A.1)). The border of the stability domain is determined by the condition $Re(\lambda) = 0$. Therefore, taking $\lambda = i\Omega$ on the stability boundary and separating real and imaginary parts, we obtain two real equations

$$\begin{aligned} f_r(\Omega, \mathcal{E}, \gamma) &= 0 , \\ f_i(\Omega, \mathcal{E}, \gamma) &= 0 . \end{aligned} \tag{2.8}$$

Both equations are linear with respect to $\mathcal{E}$ and γ. Therefore this system can be analytically resolved with respect to γ and $\mathcal{E}$ and, with the account of Eq. (2.5) and $\varepsilon_f \cos\theta = \mathcal{E}$, rewritten as

$$\begin{aligned} \theta &= \theta(\Omega) , \\ \varepsilon_f &= \varepsilon_f(\Omega) . \end{aligned} \tag{2.9}$$

These are the equations of the stability boundary in the parameter plane (θ, ε_f) in a parametric form; these lengthy expressions are given in the Appendix. Fig-

ure 2.4 shows stability domains according to Eqs. (2.16) for different values of the phase shift β and for the following values of the parameters: $\omega = 2\pi/32.5$, $\alpha = 0.3\omega$, $\mu = 500$, $\xi = 0.0048$. These parameters are chosen for comparison of the theory with the results of numerical simulation presented below. The domains quantitatively agree with the suppression domains, obtained in simulations of stimulated ensemble of all-to-all coupled Bonhoeffer - van der Pol oscillators, see Figs. 2.6,2.7 below.

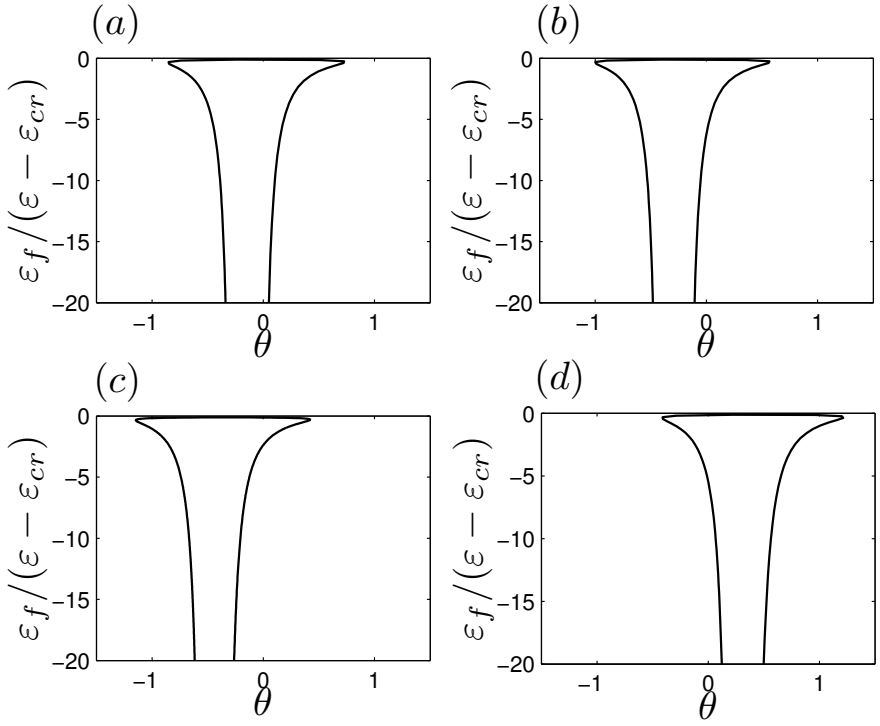

Figure 2.4: Stability domains for the model equation (2.7) for different values of β. (*a*) $\beta = 0$, (*b*) $\beta = \pi/20$, (*c*) $\beta = \pi/10$, (*d*) $\beta = -\pi/7$. The domains represent large, closed islands, which extend to large negative values of ε_f; only areas of strong stability are shown here.

2.3 Control of synchrony in neural ensembles

To demonstrate the efficiency of our technique, we start by consideration of a simple model of collective synchrony. In a population of neurons each unit usually interacts with many other units, and, therefore, the collective dynamics is

typically described by a mean-field model, which assumes a global (all-to-all) coupling between the elements. However, simulations with Rulkov neuronal model (56) show that a randomly coupled population with a rather low connectivity of about 0.5% can be with a good precision described by a mean-field model (36).

2.3.1 Bonhoeffer - van der Pol oscillators

For the introduction of collective synchrony control we consider suppression of the mean field in an ensemble of N Bonhoeffer - van der Pol oscillators, coupled via the mean field in the x variable (Eq. 2.1). The stimulation $\mathcal{C}$ is modeled by including an additional term into the r.h.s. of the Bonhoeffer - van der Pol model (2.1). However, in fact it is unknown, which variable, x or y, is affected by the stimulation. Therefore, for the generality, we assume that the stimulation is applied to both equations for x and y:

$$\begin{aligned} \dot{x}_i &= x_i - x_i^3/3 - y_i + I_i + \varepsilon X + \mathcal{C}\cos\psi \ , \\ \dot{y}_i &= 0.1(x_i + 0.7 - 0.8y_i) + \mathcal{C}\sin\psi \ , \end{aligned} \tag{2.10}$$

where the parameter ψ governs the distribution of the stimulation between two equations. Note that the parameter ψ is related but not equal to the parameter β in Eq. (2.2). Indeed, as was shown in (35), even if $\psi = 0$, in the corresponding amplitude equation for the collective oscillations near the bifurcation point there appears a phase shift β, which is generally not zero. The parameter β is determined by the organization of global coupling in the ensemble and by the properties of individual units. This parameter characterizes the *a priori* unknown phase shift, inherent to the stimulation.

We emphasize, that model (2.10) is quite general, and, though we are speaking about interacting neurons here, our method can be applied to control the dynamics of a population of limit cycle oscillators of any physical nature. On the other hand, model (2.10) lacks several important features specific for neuronal interaction. These features are considered in a more realistic model below.

We introduce the control loop via Eqs. (2.3,2.4,2.6). We simulated the system (2.10) for $N = 10000$ and internal coupling $\varepsilon = 0.03$. The parameters of the band pass filter are $\omega = 2\pi/32.5$, $\alpha = 0.3\omega$. The parameter of the integrator is $\mu = 500$. The results for $\beta = 0$, $\theta = 0$ are shown in Fig. 2.5. The control was

switched on at $t_0 = 300$, i.e., $\varepsilon_f = 0$ for $t < t_0$ and $\varepsilon_f = -0.009$ for $t \geqslant t_0$. The panels (a) and (b) present the mean field and the control signal, respectively. It is seen that the stimulation results in a rapid suppression of the collective oscillation of the ensemble, where only small noise-like fluctuations remain. We quantify the suppression by the coefficient $S = \dfrac{\mathrm{rms}(X)}{\mathrm{rms}(X_f)}$, where X and X_f are the mean fields in the absence and presence of the feedback, respectively. For the example shown in Fig. 2.5, we get $S = 157$. Generally, the suppression coefficient depends on the population size N like $S{\sim}\sqrt{N}$ (cf. (34)).

It is important that as soon as the suppression is achieved, the feedback signal practically vanishes, $\langle \mathcal{C} \rangle = -5 \cdot 10^{-6}$ and $\mathrm{rms}(\mathcal{C}) = 0.0005$, to be compared to the amplitude of individual units ≈ 1.8. The dynamics of two neurons is shown in Fig. 2.5(c). One can see that the feedback control does not affect oscillations of individual units, but just destroys the synchrony between them so that they oscillate incoherently and therefore produce no macroscopic oscillation.

To illustrate the effect of damping parameter α of the filter on suppression we present in Fig. 2.6 the dependencies of the suppression coefficient S on θ, ε_f for an ensemble of $N = 500$ Bonhoeffer - van der Pol oscillators (2.10); here $\psi = 0$. The domains, where suppression is effective, represent closed, isolated areas. From these figures we can conclude that suppression of synchrony is observed for a relatively large parameter range. One can also see that with the increase of the damping parameter α, the suppression domains increase as well.

Figure 2.7 illustrates the functioning of the phase shifter. Here we show the suppression domains $S = S(\theta, \varepsilon_f)$ for different values of the phase shift ψ (see Eq. (2.10)). For example, for $\psi = \pi/10$, the collective synchrony cannot be suppressed for $\theta = 0$, i.e., the suppression is achieved only with the help of the phase shifter.

2.3.2 Desynchronization in a model of neuronal ensemble with synaptic coupling

In this Section we make a step towards more realistic modeling of controlled neuronal dynamics. For the introductory example we used a quite abstract model (2.10); now we take into account several important features of the measurement

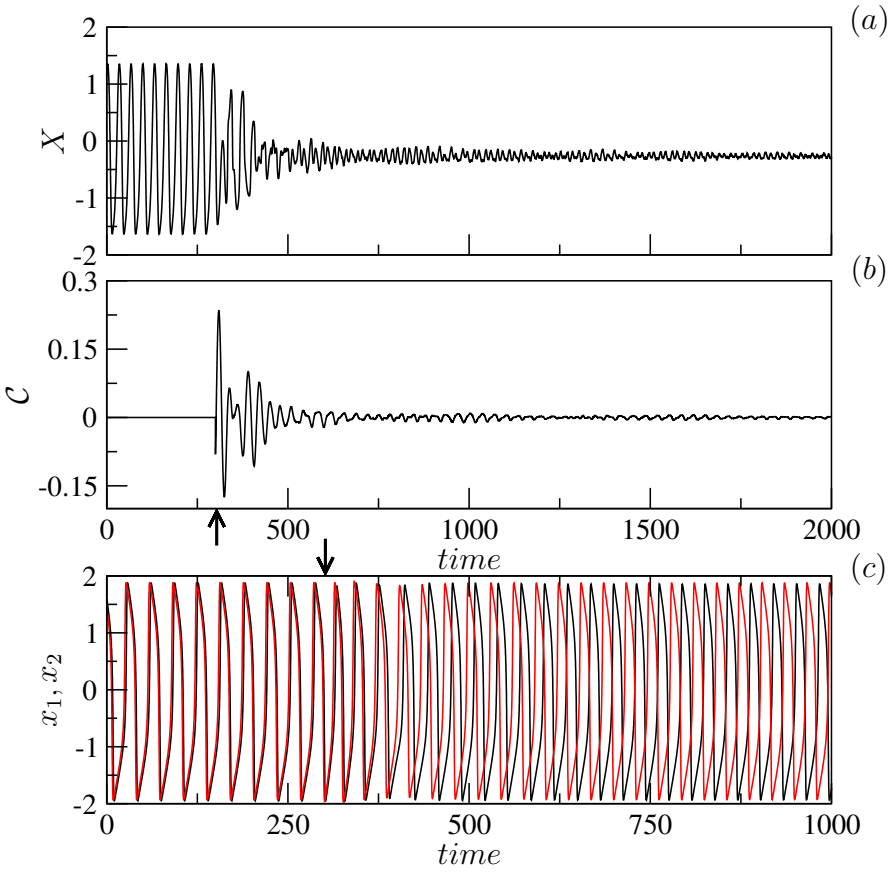

Figure 2.5: Suppression of synchrony in the population of Bonhoeffer - van der Pol oscillators, Eqs. (2.10). (a,b) The mean field X and the control signal $\mathcal{C}$ vs time. (c) Synchronous and asynchronous dynamics of two neurons in the absence and in the presence of the stimulation, respectively. The arrows indicate when the control is switched on.

of the collective neuronal activity and of the coupling between the neurons.

We have assumed that the collective activity of the population is reflected in the local field potential (LFP); the latter can be registered by an extracellular electrode. The question is how to relate the variables of conductance-based neuronal models to the LFP. The extracellular potential can be obtained via solution of the Poisson equation with the membrane currents[3] determining the boundary condition (57; 58). Thus, the potential registered by the electrode is

[3]These currents are due to the motion of ions from the extracellular space into the cells and back.

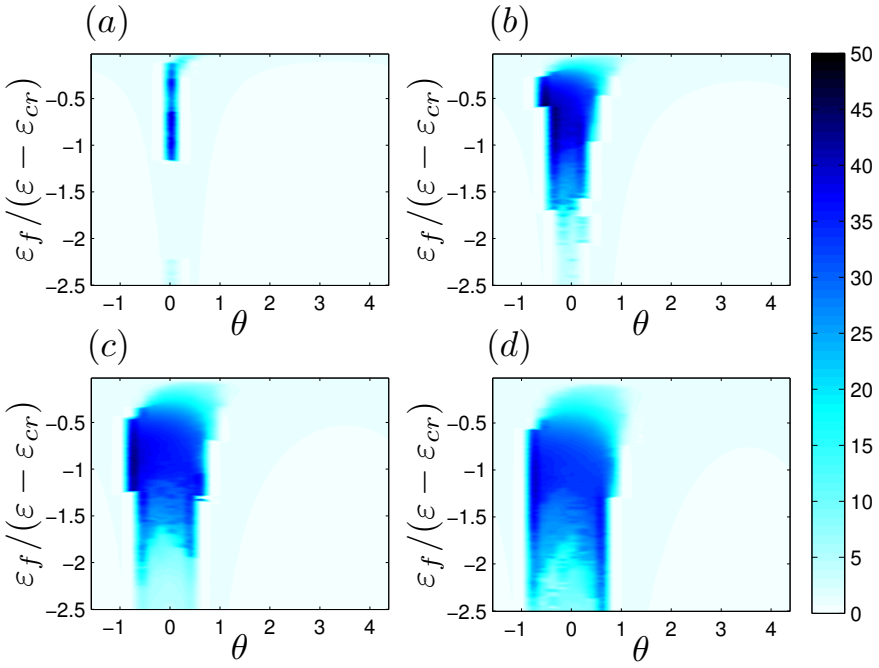

Figure 2.6: Domains of suppression for $N = 500$ Bonhoeffer - van der Pol neurons (2.10) in dependence on the damping parameter α of the oscillator (2.3). The suppression factor S is shown in a blue scale coding. (a) $\alpha = 0.1\omega$, (b) $\alpha = 0.3\omega$, (c) $\alpha = 0.5\omega$, (d) $\alpha = 0.7\omega$. Note that only the regions with relatively large suppression factor are shown: actually the stability domains extend for quite large negative values of ε_f (cf. Fig. 2.4).

$\Phi \sim \sum_i (\mathcal{I}_i/r_i)$, where r_i is the distance between the current source, i.e. the membrane current of the ith neuron $\mathcal{I}_i$, and the measuring point. Hence, in the first approximation, neglecting the spatial structure of the ensemble, we can represent the measured signal as

$$\Phi \sim \sum_i \mathcal{I}_i \ . \tag{2.11}$$

$\mathcal{I}_i$ is the right hand side of the equation for the membrane potential V_i of a conductance-based neuronal model

$$C_i \frac{dV_i}{dt} = \mathcal{I}_i \ ,$$

where C_i is the capacitance of the membrane. Note that $\mathcal{I}_i$ are the total membrane currents which contain the currents through different ion channels and

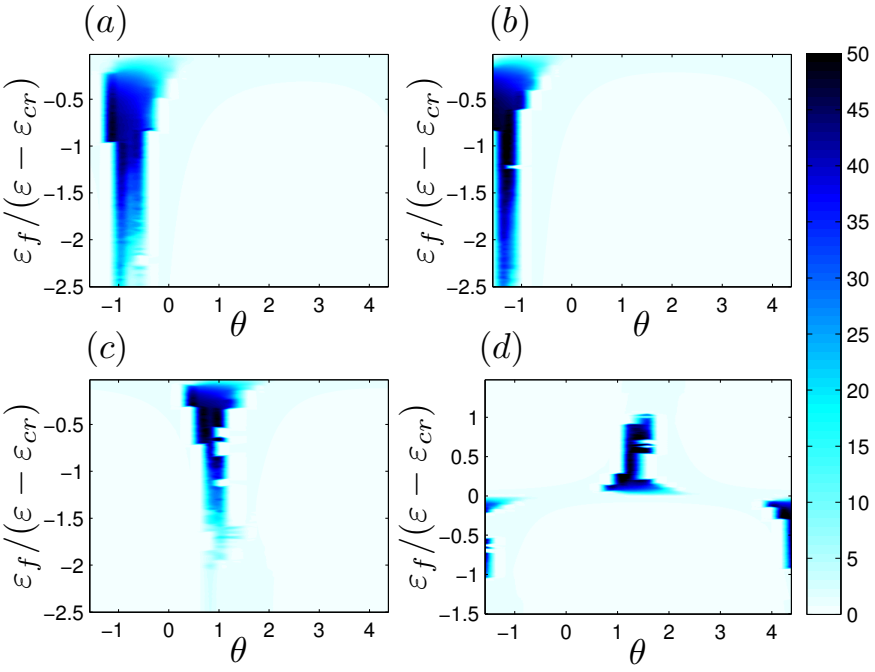

Figure 2.7: Domains of suppression for $N = 500$ Bonhoeffer - van der Pol neurons (2.10) for different values of the phase shift ψ: (a) $\psi = \pi/10$, (b) $\psi = \pi/20$, (c) $\psi = -\pi/7$, (d) $\psi = \pi/3$. These domains confirm that the phase shifter indeed ensures suppression. The damping parameter $\alpha = 0.3\omega$. These numerical results are in good agreement with theoretical results (cf. Fig. 2.4).

external currents, including the current due to stimulation. Using the notations of Eqs. 2.10, we can write $\Phi \sim \sum_i \mathcal{I}_i = \sum_i \dot{x}_i = N\dot{X}$. It means, that the stimulation is now proportional to the derivative of the mean field.

Now we explore the efficacy of suppression of collective rhythms in a neuronal ensemble with all-to-all synaptic connections. Indeed, interaction via the electrical (gap junction) coupling is possible only if the neurons are spatial neighbors[4]. Therefore, in a large network, where even spatially distant neurons can be synaptically linked by long axons, synaptic coupling plays a more important role.

Each neuron is modeled by the Hindmarsh-Rose equations (59), whereas the model and parameters of the inhibitory synaptic coupling are taken from

[4]The electrical coupling is a usual resistive coupling; it is possible only if the interacting neurons are closely spaced.

Ref. (60). Thus, the dynamics of the ensemble is described by the following set of equations:

$$\begin{aligned} \dot{x}_i &= y_i + 3x_i^2 - x_i^3 - z_i + I_i - \frac{\varepsilon}{N-1}(x_i + V_c)\sum_{j\neq i}^{N}\left[1 + e^{(x_j - x_0)/\eta}\right]^{-1} + \mathcal{C} \ , \\ \dot{y}_i &= 1 - 5x_i^2 - y_i \ , \\ \dot{z}_i &= r[\nu(x_i - \chi) - z_i] \ , \end{aligned} \tag{2.12}$$

where $r = 0.006, \nu = 1, \chi = -1.56$. ε is the strength of the synaptic coupling with the reverse potential $V_c = 1.4$; other parameters of synapses are $\eta = 0.01$, $x_0 = 0.85$. I_i is taken as $I_i = 4.2 + \sigma$, where σ is Gaussian distributed with zero mean and 0.05 rms value. For zero coupling, each neuron exhibits regular spiking. With the increase of the synaptic coupling between the neurons, the model demonstrates a transition from independent firing to coherent collective activity[5]. In the Eqs. (2.12) the variable x has the meaning of the membrane potential V. Hence, the local filed potential should be taken as $\Phi \sim \sum_i \dot{x}_i \sim \dot{X}$. It means, that the derivative of the mean field is measured and that the stimulation is now proportional to $\dot{X}$. While modeling the suppression by feedback control, we assume that the stimulation can be described as an additional external current, identical for all neurons. Therefore, the term, describing stimulation, enters the right hand side of the first equation (2.12).

The results of simulation for $N = 200$ nonidentical inhibitory coupled neurons are illustrated in Fig. 2.8. Here we show in blue-scale coding the suppression factor S as a function of the feedback strength ε_f and the phase shift θ. We remind that this shift is a free parameter of the control scheme and is intended to compensate the unknown phase shift β, inherent to stimulation. One can see that the suppression domain qualitatively is in good agreement with the theoretical result, see Fig. 2.4. The simulations have been done for the following values of the parameters: $\varepsilon = 0.15$ and $\alpha = 0.3\omega$. The average frequency of the mean field was estimated as $\omega = 2\pi/3.82$. Note that in this model the mean action on each element *is not the mean field* X. Nevertheless, the measurement of $\dot{X}$ suffice to ensure desynchronization in the ensemble.

Finally, we consider the case when individual neurons exhibit chaotic burst-

[5]The dynamics of the coherent activity is quite complicated, however, it can be suppressed.

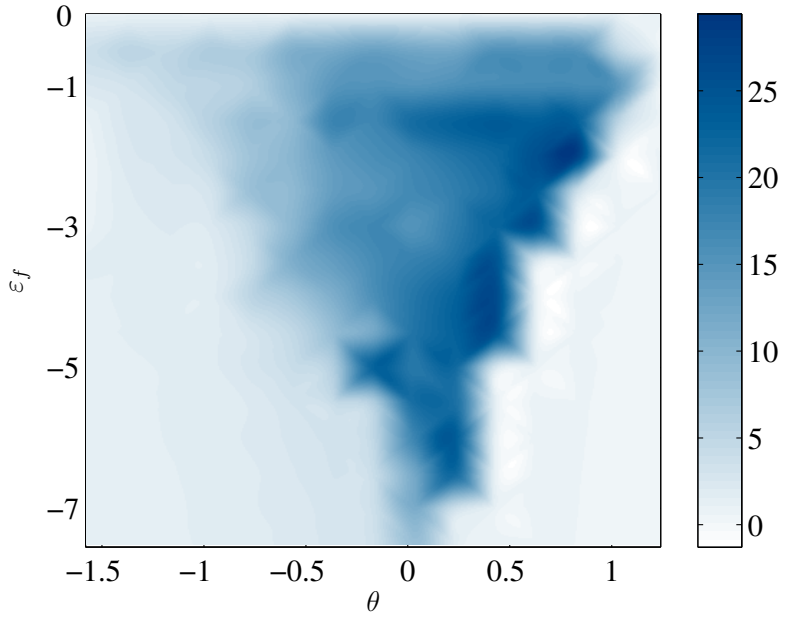

Figure 2.8: Domain of suppression for the ensemble of 200 nonidentical synaptically coupled Hindmarsh-Rose neurons (Eq. 2.12) in a regime of periodic spiking.

ing, i.e. generation of action potentials (spikes) alternates with the epochs of quiescence, so that the oscillation can be characterized by two time scales. This dynamics is provided by the Eq. (2.12) with the following set of parameters: $r = 0.006, \nu = 4, \chi = -1.6$; the parameters of coupling are kept the same as in the previous example. Synchronization occurs on the slower time scale, i.e. different neurons burst nearly at the same time, whereas the spiking within the bursts is not synchronous, and therefore is to a large extent averaged out in the mean field (Fig. 2.9b). However, some high frequency jitter remains due to correlations in spiking. As a result, the mean field is irregular; besides this jitter, it also exhibits a low frequency modulation. The (average) frequency of the mean field is $\omega = 2\pi/176$, this corresponds to the inter-burst intervals.

Figure 2.9b demonstrates that though the mean field is irregular, it has a strong periodic component and therefore we expect that our technique is efficient in this case as well. This is indeed confirmed by the results of numerical simulation for $I_i = 3.2$, $\varepsilon = 0.2$ and various values of the damping parameter α, see Fig. 2.10. We note that in order to avoid large current pulse at the beginning of the stimulation, the latter is switched on in a smooth way (Fig. 2.9a). As

in the case of spiking neurons and in agreement with the theory, for the bursting neurons the stability domains elongate for rather large negative values of ε_f. Simulations also show that the increase of the damping parameter α, i.e. the increase of the bandwidth of the filter, leads to the extension of the suppression regions, similarly to the case of periodic oscillators (cf. Fig. 2.6). We conclude that suppression is possible in case of irregular mean field as well, as long as the latter has a strong periodic component (what is expected if the system is not too far from the point of transition to synchronization). We remind, that in order to simulate the measurement of LFP we use for stimulation the derivative of the mean field. This process (Fig. 2.9c) is even more complex than X; however, the suppression is achieved.

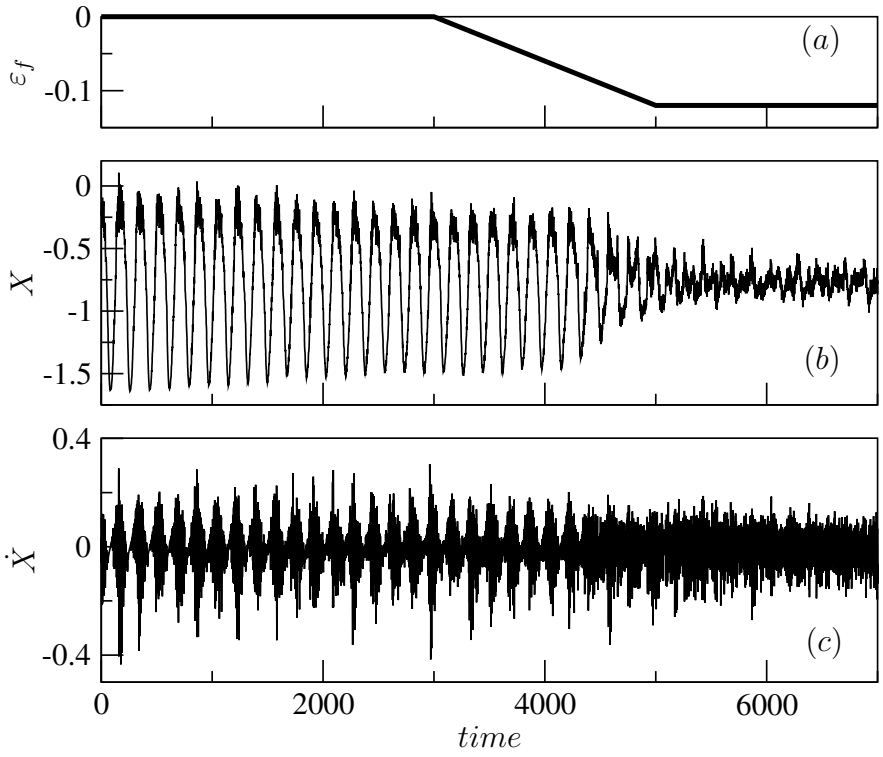

Figure 2.9: (a) Feedback control ensures suppression of collective activity in an ensemble of bursting Hindmarsh-Rose neurons. Slow switching of the stimulation helps to avoid initial large current pulse. (b) Mean field in ensemble of synaptically coupled bursting Hindmarsh-Rose neurons is irregular but has a strong periodic component. The control has been switched on smoothly between $t = 3000$ and $t = 5000$. The suppression factor is $S = 6.5$, $\varepsilon_f = -0.12$, $\theta = -1.2$, $\alpha = 0.3\omega$. Note that for the measured signal we took the derivative of the mean field, shown in (c).

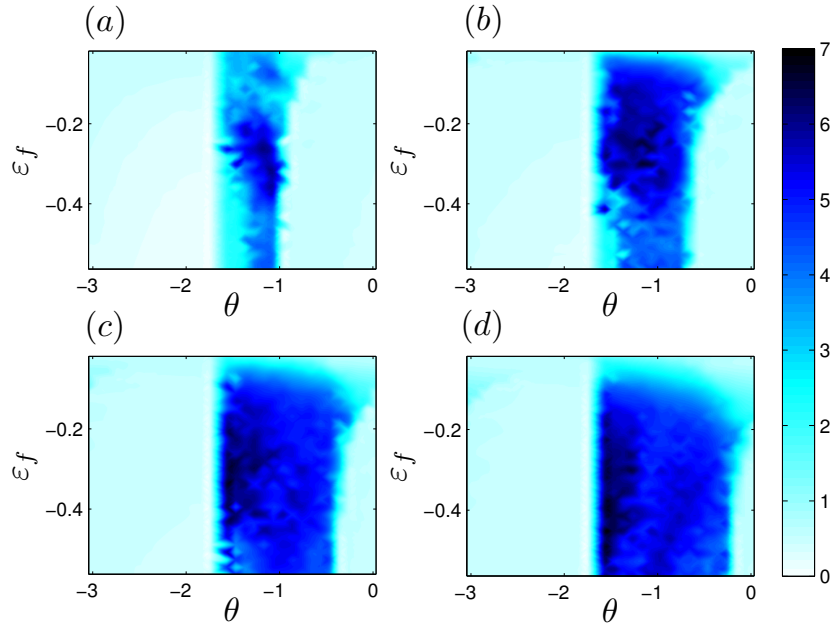

Figure 2.10: Domains of suppression for 200 bursting Hindmarsh-Rose neurons Eq. (2.12) for different values of the damping parameter α: (a) $\alpha = 0.1\omega$, (b) $\alpha = 0.3\omega$, (c) $\alpha = 0.5\omega$, (d) $\alpha = 0.7\omega$.

2.4 Suppression of synchrony in two interacting neuronal populations

As it has been demonstrated above, suppression of pathological brain rhythms in a large population of globally coupled elements can be effectively achieved by means of proposed *linear feedback* technique; we suggested that this technique can be used for suppression of pathological brain rhythms with the help of DBS. We proceed from the assumption that the collective activity of many neurons is represented in the local field potential (LFP), which can be continuously monitored in an experiment and subsequently, after a certain processing, used for stimulation of the brain tissue via a feedback loop. We also assumed, that the signal from the whole network can be registered and that the whole network can be stimulated. However, for practical applications it is important to consider the situation when the measuremental and stimulation electrodes are implanted into different, non-overlapping, though interacting, populations: the first one is affected by the stimulation, while the collective activity is registered from the second one. Generally speaking, the second population can be by itself both active and passive (below we consider both cases).

For this reason, in this Section we treat a model of two interacting globally coupled ensembles (cf. (61; 62; 36; 63)), where one population is supposed to be affected by the stimulation derived from collective activity (LFP) of the second one (see Fig. 2.11). Our requirements to the suppression technique remain the same, we just run through the main points. First, we require that as soon as the desired asynchronous state is achieved, the control signal should vanish, or, strictly speaking, should decrease to the noise level (*vanishing-stimulation control*). Next, the control scheme should be able to compensate an *a priory* unknown phase shift, inherent to stimulation. This phase shift β is determined by the way the stimulation is incorporated into model equations (note, that exact electro-physiological mechanism of stimulation is unknown) and by organization of internal coupling in the ensemble (see discussion in (35)).

The control technique should also be able to compensate latency in measurements. Another requirement is that the controller should be able to extract the relevant signal from its mixture with the rhythms produced by neighboring

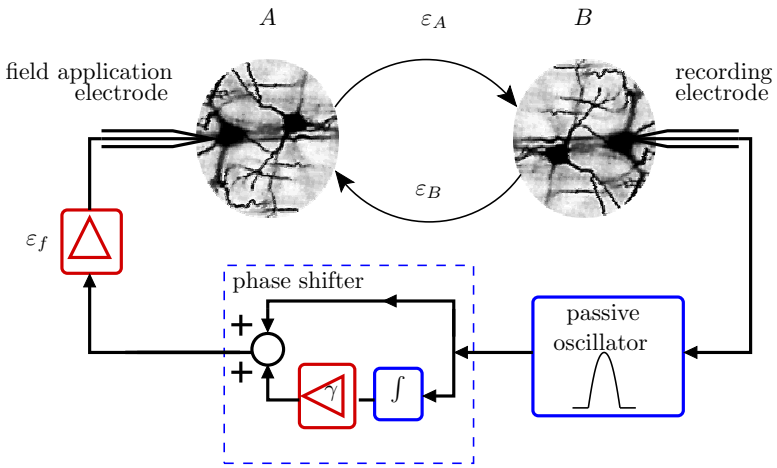

Figure 2.11: Suggested suppression scheme. The local field potential of the population B is measured by the recording electrode and is fed back via the field application electrode to the population A. The feedback loop contains a passive oscillator playing the role of a band pass filter, an integrator, a summator, and two amplifiers.

neuronal populations and with the measuremental noise.

2.4.1 Stability analysis of two interacting neuronal ensembles

Here we analyze the controlled dynamics of two interacting ensembles of neurons. It is assumed that the elements within each population are globally coupled and the interaction between these populations is of the mean field type, i.e. the mean field A of one ensemble acts on all elements of the second ensemble and, vice versa, the mean field B of the second ensemble influences all elements of the first one.

Model equations

Following the theoretical description outlined in Section 2.2 we can write two symmetrically coupled equations for the complex amplitudes A and B together

with the equations for the control loop:

$$\begin{aligned} \dot{A} &= (\xi_1 + i\omega_1)A - |A|^2 A + \varepsilon(B - A) + \mathcal{C}e^{i\beta} , \\ \dot{B} &= (\xi_2 + i\omega_2)B - |B|^2 B + \varepsilon(A - B) , \\ \ddot{u} &+ \alpha\dot{u} + \omega_0^2 u = Re(B) , \\ \mu\dot{d} &+ d = \dot{u} . \end{aligned} \tag{2.13}$$

The external stimulus administered to all elements of the first subpopulation has the same form as in Eq. (2.6), namely

$$\mathcal{C} = \pm\frac{\varepsilon_f}{\sqrt{1 + \gamma^2/\omega^2\mu^2}}(\dot{u} + \gamma d) = \varepsilon_f \cos\theta \cdot (\dot{u} - \omega\mu d \tan\theta) ,$$

where $\sqrt{1 + \gamma^2/\omega^2\mu^2} = 1/\cos\theta$ is the normalization coefficient. It ensures an independence of the amplification in the feedback loop from the phase shift θ, so that this amplification is completely determined by ε_f. At the points $\theta = \pm\pi/2$ the control term is calculated as $\mathcal{C} = \varepsilon_f\omega\mu d$. We recall that the phase shift β describes the uncertainty of our action on the active oscillator.

Similarly to the stability analysis, performed in Section 2.2 for one neural population, we neglect the nonlinear terms of Eqs. (2.13) and substitute $A = a_1 + ia_2$, $B = b_1 + ib_2$, $\dot{u} = v$ in Eq. (2.13). Writing separately the real and imaginary parts we obtain:

$$\begin{aligned} \dot{a}_1 &= \xi_1 a_1 - \omega_1 a_2 + \varepsilon(b_1 - a_1) + \mathcal{E}(v + \gamma d)\cos\beta , \\ \dot{a}_2 &= \xi_1 a_2 + \omega_1 a_1 + \varepsilon(b_2 - a_2) + \mathcal{E}(v + \gamma d)\sin\beta , \\ \dot{b}_1 &= \xi_2 b_1 - \omega_2 b_2 + \varepsilon(a_1 - b_1) , \\ \dot{b}_2 &= \xi_2 b_2 + \omega_2 b_1 + \varepsilon(a_2 - b_2) , \\ \dot{u} &= v , \\ \dot{v} &+ \alpha v + \omega_0^2 u = b_1 , \\ \mu\dot{d} &+ d = \dot{u} . \end{aligned} \tag{2.14}$$

Here we denote $\mathcal{E} = \varepsilon_f/\sqrt{1 + \gamma^2/\mu^2\omega_0^2} = \varepsilon_f \cos\theta$. Seeking the solution in the form $a_1 = A_1 e^{\lambda t}$, $a_2 = A_2 e^{\lambda t}$, $b_1 = B_1 e^{\lambda t}$, $b_2 = B_2 e^{\lambda t}$, $u = Ue^{\lambda t}$, $v = Ve^{\lambda t}$, $d = De^{\lambda t}$ we obtain the algebraic system of 7 linear equations. This system has a non-trivial solution if its determinant is equal to 0; this condition provides the equation $f(\lambda, \mathcal{E}, \gamma) = 0$. The boundary of the stability domain is determined by

the condition $Re(\lambda) = 0$. Therefore, taking $\lambda = i\Omega$ on the stability boundary and separating real and imaginary parts, we obtain two real equations

$$\begin{aligned} f_r(\Omega, \mathcal{E}, \gamma) &= 0 , \\ f_i(\Omega, \mathcal{E}, \gamma) &= 0 . \end{aligned} \tag{2.15}$$

Both equations are linear with respect to $\mathcal{E}$ and γ. Therefore this system can be analytically resolved with respect to γ and $\mathcal{E}$ and, with the account of $\theta = -\arctan\left(\frac{\gamma}{\omega\mu}\right)$ and $\varepsilon_f \cos\theta = \mathcal{E}$, rewritten as

$$\begin{aligned} \theta &= \theta(\Omega) , \\ \varepsilon_f &= \varepsilon_f(\Omega) . \end{aligned} \tag{2.16}$$

These are the equations of the stability boundary in the parameter plane (θ, ε_f) in a parametric form. This system has been solved by using the same algorithm as in Sec. 2.2. Since dimension of the system in this case is equal to 7 we skip here all these very lengthy expressions, but provide the code, by means of which this system has been solved (see Appendix B).

Different regimes can be implemented by choosing appropriate values of frequencies $\omega_{1,2}$ and increments $\xi_{1,2}$. Let us consider first the case of two interacting identical subsystems ($\omega_1 = \omega_2 = \omega_0 = 1.0$, $\xi_1 = \xi_2 = 0.02$). The stability domain in the parameter plane (θ, ε), i.e. the region, where the control is efficient for this case, is presented in Fig. 2.12a. Second, we take two nonidentical populations: $\omega_1 = 1.0$, $\omega_2 = 1.04$, $\omega_0 = 1.0$. The results show (see Fig. 2.12b) that suppression can be achieved in this case as well. Finally, we model a situation when the population, from which LFP is measured, is by itself stable ($\xi_2 < 0$). This may reflect the case when the recording electrode is placed rather far from the region of pathological activity, e.g., on the surface of the scalp. We illustrate this case in Fig. 2.12c.

2.4.2 Numerical example: two coupled Bonhoeffer - van der Pol populations

To compare the above obtained results of theoretical analysis with the results of numerical stimulation, we consider two interacting ensembles of N globally

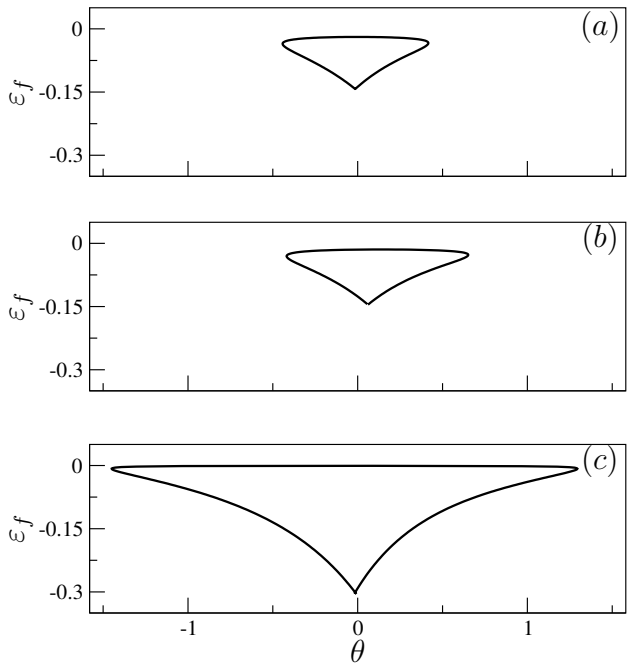

Figure 2.12: Stability domains for the model equation (2.13) for the case of identical (a) and nonidentical (b) subpopulations. Panel (c) represents the case, when the population B, where the measurement is performed, is stable ($\xi_2 = -0.02$). The other parameters are: $\varepsilon = 0.05$, $\alpha = 0.3\omega_0$, $\mu = 500$, $\beta = 0$.

coupled Bonhoeffer - van der Pol oscillators:

$$\begin{aligned}
\dot{x}_{Ai} &= x_{Ai} - x_{Ai}^3/3 - y_{Ai} + I_{Ai} + \varepsilon_A X_A + \mathcal{K}(X_B - X_A) + \mathcal{C}\cos\psi \ , \\
\dot{y}_{Ai} &= 0.1(x_{Ai} + 0.7 - 0.8y_{Ai}) + \mathcal{C}\sin\psi \ , \\
\dot{x}_{Bi} &= x_{Bi} - x_{Bi}^3/3 - y_{Bi} + I_{Bi} + \varepsilon_B X_B + \mathcal{K}(X_A - X_B) \ , \\
\dot{y}_{Bi} &= 0.1(x_{Bi} + 0.7 - 0.8y_{Bi}) \ , \\
\ddot{u} &+ \alpha\dot{u} + \omega_0^2 u = X_B \ , \\
\mu\dot{d} &+ d = \dot{u} \ ,
\end{aligned} \tag{2.17}$$

where two last equations describe the feedback loop. The oscillators within each ensemble are globally coupled via the mean fields $X_{A,B} = N^{-1}\sum_i x_{Ai,Bi}$, with the internal coupling strengths ε_A and ε_B; $i = 1, \ldots, N$ is the index of the neuron.

Parameters $I_{Ai,Bi}$ have the meaning of the external current and directly influence the spiking frequency of elements of both ensembles. In our case oscillators are not identical: $I_{Ai} = 0.6 + \sigma$, $I_{Bi} = 0.62 + \sigma$, where σ is a Gaussian distributed number with zero mean and 0.1 rms value. The external stimulus administered to all elements of first population is modeled by including an additional term into the r.h.s. of the Bonhoeffer - van der Pol equations and has the same form as in Eq. (2.6). Parameter ψ describes the uncertainty of how stimulation enters the equations. We remind that the parameter ψ is related but not equal to the parameter β in Eq. (2.13).

The results of simulation for $N = 10000$ oscillators in each population are shown in Fig. 2.13 for the following set of parameters: internal coupling $\varepsilon_A = \varepsilon_B = 0.03$, $\mathcal{K} = 0.1$, and $\psi = 0$, $\theta = 0.03$. The parameters of the band pass filter and integrator are: $\omega_0 = 2\pi/32.5$, $\mu = 500$. Here again we chose the damping factor of the oscillator as $\alpha = 0.3\omega_0$, reasoning from the knowledge of the Parkinsonian rhythm band pass from 10 to 13 Hz.

The panel 2.13a presents the mean field dynamics of the subsystems A and B. The control signal is switched on at $t_0 = 400$, i.e., $\varepsilon_f = 0$ for $t < t_0$ and $\varepsilon_f = -0.012$ for $t \geqslant t_0$ (see Fig. 2.13b). Switching on the stimulation leads to the desynchronization in both subpopulations. The suppression is characterized by

$$S_{A,B} = \frac{\mathrm{rms}(X_{A,B})}{\mathrm{rms}(X_{A_f,B_f})} \ ,$$

where $X_{A,B}$ and X_{A_f,B_f} are the mean fields in the absence and presence of the feedback, respectively. For this particular example we get $S_A = 149, S_B = 143$. Figure 2.13 demonstrates two main properties of our feedback scheme: (i) as soon as desired suppression is achieved the measured mean field X_B tends to zero and thus the feedback signal practically vanishes, i.e $\langle \mathcal{C} \rangle = 1.3 \cdot 10^{-7}$ and $\mathrm{rms}(\mathcal{C}) = 0.001$; (ii) the stimulation does not effect the natural oscillatory dynamics of individual neurons. It is seen from Fig. 2.13, where dynamics of two neurons is presented in the absence (Fig. 2.13c) and in the presence (Fig. 2.13d) of the control. Individual neurons continue oscillating as before, but not coherently. In biological terms, this would mean suppression of the tremor-related brain activity with a minimal intervention into the neural tissue that does not destroy individual units.

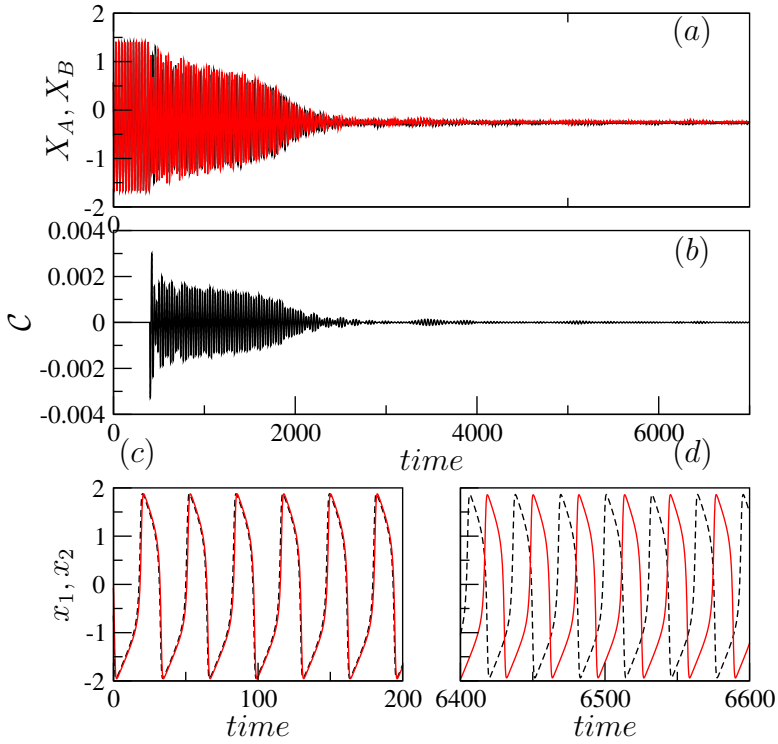

Figure 2.13: Suppression of synchrony in two coupled Bonhoeffer - van der Pol subpopulations (Eqs. (2.17)). (a) The mean fields of these subpopulations (X_A, X_B) without ($t < 500$) and with ($t > 500$) an external feedback. (b) The control signal $\mathcal{C}$ vs time. (c), (d) Synchronous and asynchronous dynamics of two neurons in the absence and in the presence of the stimulation, respectively.

For the quantitative comparison of the theoretical description within the framework of the model equation (2.13) with the numerics we simulate $N = 500$ Bonhoeffer - van der Pol oscillators (2.17) in each population and plot in a color-scale coding suppression coefficients S_A (Fig. 2.14a) and S_B (Fig. 2.14b) as a function of the phase shift θ and the feedback strength ε_f. The dark red color corresponds to the maximum suppression factor S. In this case each ensemble in the absence of control produces macroscopic mean field ($\varepsilon_{A_f,B_f} > \varepsilon_{cr}$), or in other words, both ensembles are active. The parameters of ensembles and feedback control are taken as in the previous example (Fig. 2.13). These domains of suppression have to be compared with theoretically obtained stability regions in the case of two nonidentical populations (see Fig. 2.12b). The case when the

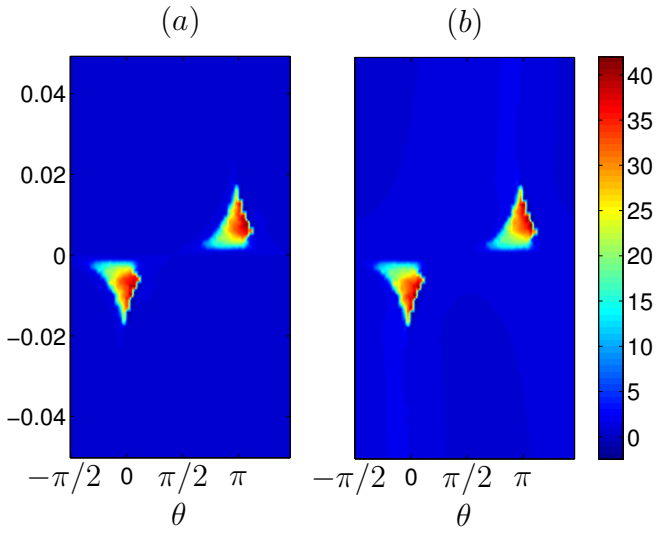

Figure 2.14: Domains of suppression for two active coupled Bonhoeffer - van der Pol ensembles (2.17). Each population consists of $N = 500$ oscillators. The suppression factor is shown in a color-scale coding: (a) the suppression factor S_A of the stimulated population A, (b) the suppression factor S_B of the measured population B.

stimulated population produces non-zero macroscopic mean field, i.e., the population is active, $\varepsilon_{A_f} > \varepsilon_{cr}$, whereas the monitored population is passive, $\varepsilon_{B_f} < \varepsilon_{cr}$, is presented in Fig. 2.15. As it is seen from this picture, the obtained suppression domains are larger then in the previous case (Fig. 2.14), that quantitatively corresponds to the theoretical results illustrated in Fig. 2.12c.

Another way to compare the theoretical analysis with the numerics is presented in Figs. 2.16, 2.17. Here we first compute the variance of the mean field for $N = 500$ elements in both subpopulations. Then, we estimate the variance of the mean field for subcritical coupling to be 0.0075; this value corresponds to the level of noise in the system. We use this value as a cutoff level: if the variance of the mean field is larger than this value, the system is considered to be unstable. The obtained stability domains are shown in Fig. 2.16 for the case when both systems are active and in Fig. 2.17 for the case when one system is active and another one is passive. The results demonstrate a good correspondence between the theory and numerics.

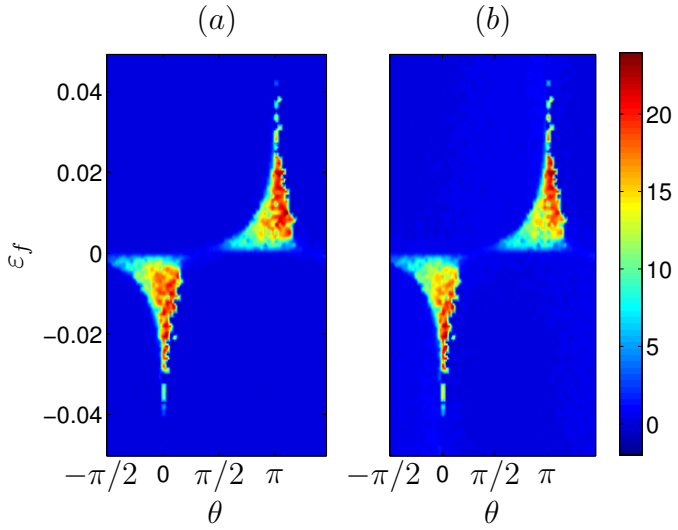

Figure 2.15: Domains of suppression for two coupled Bonhoeffer - van der Pol ensembles (2.17). Each population consists of $N = 500$ oscillators. The suppression factor is shown in a color-scale coding: (a) the suppression factor S_A of the active stimulated population A ($\varepsilon_{A_f} > \varepsilon_{cr}$), (b) the suppression factor S_B of the passive measured population B ($\varepsilon_{B_f} < \varepsilon_{cr}$).

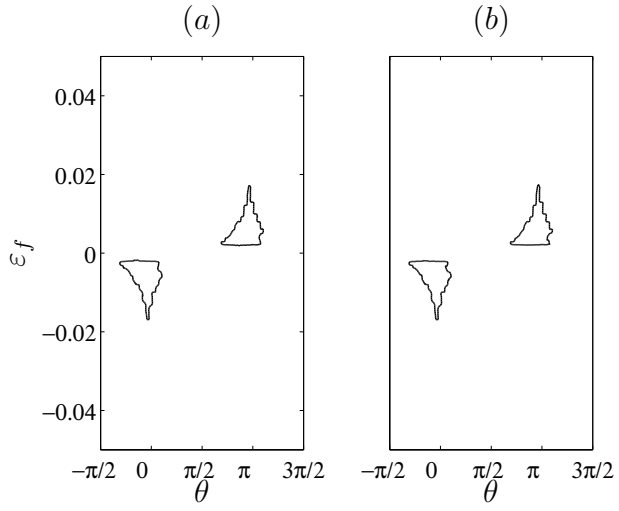

Figure 2.16: Results of numerical analysis of the stability domains of the two coupled Bonhoeffer - van der Pol ensembles (2.17). The case of two coupled active populations is presented here: (a) the stimulated population A, (b) the monitored population B.

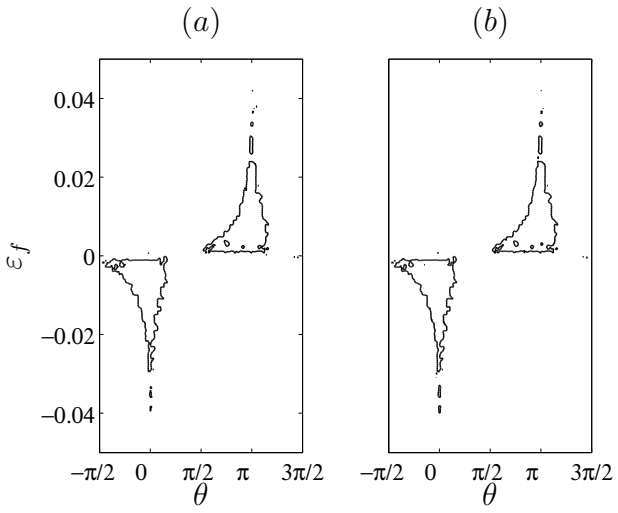

Figure 2.17: Results of numerical analysis of the stability domains of the two coupled Bonhoeffer - van der Pol ensembles (2.17). (a) the stimulated population A is active, (b) the monitored population B is passive.

2.5 Determination of stimulation parameters by a test stimulation

The presented suppression scheme has two parameters to be determined, namely the feedback strength ε_f and the phase shift θ. The parameter θ is related to the phase shift β, which is inherent to stimulation. We recall that the phase shift θ is a free parameter of our control scheme and it has been introduced with the purpose to compensate the unknown phase shift β, inherent to the stimulation. To find the appropriate parameters for an efficient stimulation one has to estimate the phase shift β. Here we introduce the simple way how this can be done in an experiment.

Suppose first that we deal with one population only. For the determination of the unknown parameter β we make use of a general property of oscillators, namely of their ability to be synchronized by a weak external forcing. Considering the population as one oscillator, we stimulate it by a harmonic force with the same frequency as its collective oscillation, i.e $\mathcal{C} = \varepsilon_f \cos(\omega t)$, and examine the entrained oscillation. (Note that in this setup we deal with an open loop system.) If the phase shift β were zero, the oscillator and the force would be in-phase.

Otherwise, the difference of the oscillator phase and phase of the force will be $\phi_{osc}-\phi_{force}=\beta$. Accordingly, at first the frequency of the uncontrolled oscillation ω has to be measured and then the proper test signal $\mathcal{C}=\varepsilon_f\cos(\omega t)$ has to be applied. The unknown parameter β can be calculated by virtue of Fourier transformation for this frequency, i.e.

$$\tilde{\beta}=-\arg\left(T_s^{-1}\int_0^{T_s}X(t)e^{i\omega t}dt\right)\ , \tag{2.18}$$

where T_s is the time of stimulation.

To validate this method for the case of two coupled ensembles, we simulated Eqs. (2.13). In order to compare the obtained results with the results of stability analysis of Section 2.2, we consider three different cases. First, we take two identical ensembles ($\omega_1=\omega_2=1.0, \xi_1=\xi_2=0.02$) with the parameters $\varepsilon=0.05$, $\varepsilon_f=0.07$, $\beta=0$; as a result we obtain $\tilde{\beta}=-6\cdot10^{-5}$. In the case of nonidentical ensembles, $\omega_1=1.0$, $\omega_2=1.04$, we obtain $\tilde{\beta}=0.11$. Finally, in the case when one system is active and the second one is passive, $\xi_1=0.02$, $\xi_2=-0.02$) we obtain $\tilde{\beta}=0.08$. Thus, in all cases the estimated values are very close to the true value $\beta=0$ and are in a good correspondence with the optimal value of the phase shift (see Fig. 2.12).

2.6 Summary and discussion

In this chapter we have considered in detail the suppression of the mean field in an ensemble of oscillators from the viewpoint of a possible application in neuroscience. In particular, we have proposed an efficient and simple technique for control of synchrony in a population of globally coupled elements. Though we have concentrated on the problem of desynchronization, the technique can be also used for excitation of collective oscillation, if the coupling in the ensemble is subcritical and, thus, the uncontrolled system is stable. The suppression or excitation can be achieved if the total phase shift provided by the feedback loop is π or zero, respectively.

We begin with the consideration of one isolated population of globally coupled neurons. Then, we have extended our non-delayed feedback approach for

control of synchrony in a population of globally coupled elements to a more complex setting of two interacting populations, where the first one is affected by the stimulation, whereas the measurement is performed from the second one. The considered situation can model suppression of pathological rhythm when registration and stimulation of the brain tissue cannot be carried out by the same or closely placed electrode(s). We have considered the cases when the second population is either active or passive; the latter case may describe the measurements by a surface electrode. We have shown that our control technique provides a vanishing-stimulation suppression, and thus reduces the invasion into the system, what is a crucial property for possible applications in neuroscience. The theoretical analysis of suppression in a system of two interacting ensembles has been done in the framework of the model amplitude equations and the results are in a good agreement with numerical simulations.

We hope that our technique can be used for manipulation of neuronal rhythms, at least in an isolated population of neurons. This is confirmed by numerical simulations of a model of neuronal population. Important advantages of the technique are the simplicity of its practical implementation, built-in band pass filter, and the ability to compensate the phase shift inherent to stimulation of the ensemble. We emphasize, that with our method we are able to stabilize the unknown steady state of the ensemble, which can also drift with time, and to maintain it by vanishingly small stimulation (cf. (54; 55; 49)). No knowledge of the properties of individual units and coupling between them is required. Finally, we remark that the latency in the measurement can be easily compensated by the phase shifter.

Chapter 3

Controlling oscillator coherence by a linear feedback

The problem, addressed in this chapter is control of a complex irregular motion, in particular, an adjustment of the coherence of a noisy or chaotic self-oscillatory system in a desirable manner. Coherence, that is to say, persistence of oscillation frequency is an essential property of self-oscillating systems and it plays a key role in the construction of clocks, electronic generators, lasers, etc. Another important characteristic of the coherence is that it determines the predisposition of an oscillatory system to synchronization (64). This is a very significant property, since the synchronization is a very wide-spread phenomena. The coherence of a noisy limit cycle oscillator in the context of phase dynamics is evaluated by the phase diffusion constant, which is in its turn proportional to the width of the spectral peak of oscillations. It is known, that many chaotic oscillators can be described within the framework of phase dynamics; therefore their coherence can be also quantified by way of the phase diffusion constant (64). The influence of the external delayed feedback on a coherence of stochastic limit cycle systems and deterministic chaotic ones has been addressed in (18; 19) for a single delayed feedback and for a multiple delayed feedback as well (20). It was analytically derived and numerically proved that the coherence of noisy or chaotic self-sustained oscillators is essentially controlled by an external delayed feedback. The main difficulty faced in (18; 19) was that in the case of delay the process is non-Markovian and that is why the well-established tools like the Fokker-Planck

formalism cannot be applied, as in the Markovian case. For this purpose, ad hoc statistical method (Gaussian approximation) has been developed. In turn, we consider here more general case, namely, the coherence control of a noisy or chaotic self-sustained oscillators is implemented by a *general linear feedback,* what includes, in particular, a linear delayed feedback.

3.1 Basic phase model

We begin with the theoretical description of the effect of a linear feedback control on noisy self-sustained oscillators. As a model we take noisy van der Pol oscillator in the case of small nonlinearity $\mu \ll 1$:

$$\begin{aligned} \dot{x} &= \Omega_0 y \,, \\ \dot{y} &= -\Omega_0 x + \mu(1-x^2)y + \frac{\varepsilon}{\Omega_0}\widehat{L}(x) + \frac{1}{\Omega_0}\zeta(t) \,, \qquad \langle \zeta(t)\zeta(t')\rangle = 2d^2\delta(t-t') \,. \end{aligned} \tag{3.1}$$

The general theory states (see, e.g., (47)) that in the first approximation external force acting on a limit cycle oscillator affects the phase variable, but not the amplitudes, because the phase is free and can be adjusted by a very weak action. For further consideration we relay on this statement and use the so-called phase description, which is valid for small noise and feedback. The van der Pol model for small nonlinearity μ and in the absence of noise and control ($d = \varepsilon = 0$) has a limit cycle solution $x_0 \approx 2\cos\phi$, $\dot{x}_0 \approx -2\Omega_0 \sin\phi$ with a uniformly growing phase $\phi(t) \approx \Omega_0 t + \phi_0$ (65). Under the influence of noise and in the absence of feedback ($d > 0$, $\varepsilon = 0$), $\phi(t)$ diffuses according to $\langle(\phi(t) - \langle\phi(t)\rangle)^2\rangle \propto D_0 t$. The uncontrolled diffusion constant D_0 is proportional to the intensity of noise d^2. The control term is presented by the linear differential operator $\widehat{L}(x)$, which can be expressed in terms of Green's function $G(t-t')$ as $\widehat{L}(x) = \int\limits_{-\infty}^{t} G(t-t')x(t')dt'$. According to (47; 64; 18; 19) we can apply the standard procedure to derive the phase equation, i.e.,

$$\dot{\phi} = \Omega_0 + \frac{\partial\phi}{\partial y_0}\Big(\frac{\varepsilon}{\Omega_0}\widehat{L}(x_0) + \frac{1}{\Omega_0}\zeta(t)\Big) \,,$$

where $x_0 = 2\cos\phi$, $y_0 = -2\sin\phi$ are the limit cycle solutions; the phase $\phi = -\arctan(y_0/x_0)$ and therefore $\dfrac{\partial\phi}{\partial y_0} = -\dfrac{x_0}{x_0^2 + y_0^2}$. Substituting the variables x_0, y_0

on the r.h.s. by ϕ we obtain

$$\dot{\phi}(t) = \Omega_0 - \frac{\varepsilon}{2\Omega_0}\widehat{L}(x_0)\cos\phi(t) - \frac{1}{2\Omega_0}\zeta(t)\cos\phi(t)\ . \tag{3.2}$$

In terms of Green's function we can write

$$\dot{\phi}(t) = \Omega_0 - \frac{\varepsilon}{\Omega_0}\int\limits_{-\infty}^{t} G(t-t')\cos\phi(t')\cos\phi(t)dt' - \frac{1}{2\Omega_0}\zeta(t)\cos\phi(t)\ . \tag{3.3}$$

Next, we average the r.h.s. over the period of oscillations and by using $\langle\cos\phi(t)\cos\phi(t')\rangle = \frac{1}{2}\cos(\phi(t') - \phi(t))$, obtain

$$\dot{\phi} = \Omega_0 - \frac{1}{2\Omega_0}\zeta(t)\cos\phi(t) - \frac{\varepsilon}{2\Omega_0}\int\limits_{-\infty}^{t} G(t-t')\cos(\phi(t') - \phi(t))dt'.$$

We use the fact that ζ is delta-correlated and independent of ϕ, so that

$$\langle\zeta(t)\zeta(t')\cos\phi(t)\cos\phi(t')\rangle \approx \langle\zeta(t)\zeta(t')\rangle\,\langle\cos\phi(t)\cos\phi(t')\rangle = d^2\delta(t-t')\ .$$

Finally, we obtain the basic phase equation

$$\dot{\phi} = \Omega_0 + a\int\limits_{-\infty}^{t} G(t-t')\cos(\phi(t') - \phi(t))dt' + \xi(t)\ , \tag{3.4}$$

where $a = -\frac{\varepsilon}{2\Omega_0}$ and $\xi(t)$ is the effective noise satisfying $\langle\xi(t)\xi(t')\rangle = \frac{d^2}{4\Omega_0^2}\delta(t-t')$.

It is important to note, that in spite of the fact that this equation has been obtained for the van der Pol oscillator (3.1), similar phase equation can be derived for any limit cycle oscillator under a weak perturbation. An additional point to emphasize is that since the phase dynamics of many chaotic oscillators is qualitatively similar to the dynamics of noisy periodic oscillators (see Ref.(64)), Eq. (3.4) can also describe phase dynamics for chaotic oscillators in the presence of the feedback loop.

Our main goal is to investigate the diffusion properties of the phase. For this purpose we split the phase into an average growth and fluctuations, namely, $\phi = \Omega t + \psi$. Then, for the fluctuating instantaneous frequency $v(t) = \dot{\psi}$, satisfying

$\langle v \rangle = 0$, from Eq. (3.4) we obtain

$$v(t) = \Omega_0 - \Omega + \xi(t) + a \int_{-\infty}^{t} G(t-t') \cos(\Omega(t'-t)) \cos(\psi(t') - \psi(t)) dt'$$
$$-a \int_{-\infty}^{t} G(t-t') \sin(\Omega(t'-t)) \sin(\psi(t') - \psi(t)) dt'. \quad (3.5)$$

3.1.1 Noise-free case

Let us first consider a noise-free case, $\xi = \psi = v = 0$. Then Eq. (3.5) reduces to

$$\Omega - a \int_{-\infty}^{t} G(t-t') \cos(\Omega(t'-t)) dt' = \Omega_0 \ .$$

Making the change of variables $t - t' = \tau$, we can write

$$\Omega - a \int_{0}^{\infty} G(\tau) \cos \Omega\tau d\tau = \Omega_0 \ . \quad (3.6)$$

It is seen from the Eq. (3.6) that the presence of the linear feedback changes oscillator frequency. Furthermore, the Eq. (3.6) provides either a unique or multiple solutions for Ω. It is difficult to analyze the latter case, and it will be considered elsewhere. In the following we choose the parameters in a way that no multistability occurs.

3.1.2 Linear approximation

Here we assume that the fluctuations of the phase are weak, i.e.
$\psi(t) - \psi(t-\tau) \ll 2\pi$. From Eq. (3.5) with account of Eq. (3.6) we get

$$v(t) = -a \int_{-\infty}^{t} G(t-t') \sin\Big(\Omega(t'-t)\Big)\Big(\psi(t') - \psi(t)\Big) dt' + \xi(t) \ ,$$

and, substituting $t - t' = \tau$, rewrite

$$v(t) = a \int_{0}^{\infty} G(\tau) \sin \Omega\tau \Big(\psi(t-\tau) - \psi(t)\Big) d\tau + \xi(t) \ , \quad (3.7)$$

where Ω is the solution of Eq. (3.6). Applying Fourier transform to Eq. (3.7), we obtain:

$$F_v(\omega) = a \int_0^\infty G(\tau) \sin \Omega\tau (F_\psi(\omega) e^{-i\omega\tau} - F_\psi(\omega)) d\tau + F_\xi(\omega) \ ,$$

or

$$F_v(\omega) = \frac{a}{i\omega} \int_0^\infty G(\tau) \sin \Omega\tau F_v(\omega) (e^{-i\omega\tau} - 1) d\tau + F_\xi(\omega) \ ,$$

$$F_v(\omega) = \frac{F_\xi(\omega)}{1 - \frac{a}{i\omega} \int_0^\infty G(\tau) \sin \Omega\tau (e^{-i\omega\tau} - 1) d\tau} \ ,$$

where $v(t) = \int_{-\infty}^{\infty} F_v(\omega) e^{-i\omega t} d\omega$, $\xi(t) = \int_{-\infty}^{\infty} F_\xi(\omega) e^{-i\omega t} d\omega$. The power spectrum of frequency fluctuations $S_v(\omega)$ is related to the power spectrum of noise $S_\xi(\omega)$:

$$S_v(\omega) = \frac{S_\xi(\omega)}{\left| 1 + \frac{a}{i\omega} \int_0^\infty G(\tau) \sin \Omega\tau (e^{-i\omega\tau} - 1) d\tau \right|^2} \ .$$

Considering the limit $\omega \to 0$ we obtain for the power spectrum of frequency fluctuations $S_v(0)$:

$$S_v(0) = \frac{S_\xi(0)}{\left| 1 + a \int_0^\infty G(\tau) \tau \sin \Omega\tau d\tau \right|^2} \ .$$

As a result, the general expression for the diffusion constant $D = 2\pi S_v(0)$ in the linear approximation is

$$D = \frac{D_0}{\left[1 + a \int_0^\infty G(\tau) \tau \sin \Omega\tau d\tau \right]^2} \ , \tag{3.8}$$

where $D_0 = 2\pi S_\xi(0)$ is the diffusion in the absence of the control.

3.1.3 Gaussian approximation

To perform statistical analysis analytically we make an assumption that the phase fluctuations $\psi(t)$ are Gaussian. We also assume the noisy term $\xi(t)$ to be Gaussian. After averaging Eq. (3.5) over the fluctuations of $v(t) = \dot{\psi}$ (which are also

Gaussian distributed), we obtain for the mean frequency Ω:

$$0 = \Omega_0 - \Omega + a \int_{-\infty}^{t} G(t-t') \cos \Omega(t'-t) \langle \cos(\psi(t') - \psi(t)) \rangle dt' \,, \tag{3.9}$$

The phase difference $\psi(t') - \psi(t) = \eta(t)$ is Gaussian, hence $\langle \cos \eta \rangle = \exp[-\langle \eta^2 \rangle / 2]$. The phase difference η can be represented as an integral of the instantaneous frequency:

$$\eta(t) = -\int_{t'}^{t} v(s) ds \,. \tag{3.10}$$

With the account of Eq. (3.10) we can rewrite Eq. (3.9) as

$$0 = \Omega_0 - \Omega + a \int_{-\infty}^{t} dt' G(t-t') \cos \Omega(t'-t) \langle \cos(\int_{t'}^{t} v(s) ds) \rangle \,.$$

Direct substitution $\tau = t - t'$, $z = s - t$ yields

$$0 = \Omega_0 - \Omega + a \int_{0}^{\infty} d\tau \cos \Omega\tau G(\tau) \langle \cos(\int_{-\tau}^{0} v(t+z) dz) \rangle \,,$$

$$0 = \Omega_0 - \Omega + a \int_{0}^{\infty} d\tau \cos \Omega\tau G(\tau) e^{-\frac{1}{2} \langle [\int_{-\tau}^{0} v(t+z) dz]^2 \rangle} \,. \tag{3.11}$$

For the variance of the phase difference η we obtain:

$$\langle \eta^2 \rangle = \langle [\int_{-\tau}^{0} v(t+z) dz]^2 \rangle = \langle \int_{-\tau}^{0} v(t+t') dt' \int_{-\tau}^{0} v(t+t'') dt'' \rangle =$$
$$\int_{-\tau}^{0} dt' \int_{-\tau}^{0} dt'' V(t''-t') = 2 \int_{-\tau}^{0} (\tau - t') V(t') dt' \equiv 2R \,, \tag{3.12}$$

where $V(t') = \langle v(t) v(t+t') \rangle$ is the autocorrelation function of the instantaneous frequency. Substituting Eq. (3.12) into Eq. (3.11) we obtain:

$$0 = \Omega_0 - \Omega + a \int_{0}^{\infty} d\tau \cos \Omega\tau G(\tau) e^{-R} \,. \tag{3.13}$$

Note, that the obtained equation is similar to Eq. (3.6), but contains an additional factor e^{-R}.

Rewriting Eq. (3.5) with the account of Eq. (3.10) and substituting $\tau = t - t'$, $z = s - t$, we obtain:

$$v(t) = \Omega_0 - \Omega + \xi(t) + a\int_0^\infty d\tau \cos\Omega\tau G(\tau) \cos\left[\int_{-\tau}^0 dz v(z+t)\right] \\ -a\int_0^\infty d\tau \sin\Omega\tau G(\tau) \sin\left[\int_{-\tau}^0 dz v(z+t)\right] . \quad (3.14)$$

In order to obtain equations for the autocorrelation function $V(t')$, we introduce the autocorrelation function of the noise $K_\xi(t')$ and the cross-correlation function $K_\xi v(t')$, i.e.,

$$K_{\xi v}(t') = \langle \xi(t+t')v(t)\rangle, K_\xi(t') = \langle \xi(t+t')\xi(t)\rangle.$$

Multiplying Eq. (3.14) by $\xi(t+t')$, $v(t+t')$ and averaging, we obtain the equations for the correlation functions $K_{\xi v}(t')$ and $K_v(t')$

$$K_{\xi v}(t') = K_\xi(t') + a\int_0^\infty d\tau \cos\Omega\tau G(\tau)\langle \xi(t+t') \cos\left[\int_{-\tau}^0 dz v(z+t)\right]\rangle \\ -a\int_0^\infty d\tau \sin\Omega\tau G(\tau)\langle \xi(t+t') \sin\left[\int_{-\tau}^0 dz v(z+t)\right]\rangle , \quad (3.15)$$

$$K_v(t') = K_{\xi v}(-t') + a\int_0^\infty d\tau \cos\Omega\tau G(\tau)\langle v(t+t') \cos\left[\int_{-\tau}^0 dz v(z+t)\right]\rangle \\ -a\int_0^\infty d\tau \sin\Omega\tau G(\tau)\langle v(t+t') \sin\left[\int_{-\tau}^0 dz v(z+t)\right]\rangle . \quad (3.16)$$

For averaging Eqs. (3.15) and (3.16) we use the Furutsu-Novikov formula, valid for zero-mean Gaussian variables x, y:

$$\langle xF(y)\rangle = \langle F'(y)\rangle\langle xy\rangle .$$

Thus, all terms having the form $\langle x \cos y \rangle$ vanish, whereas all terms of type $\langle x \sin y \rangle$ remain:

$$\langle \xi(t+t') \sin \left[\int_{-\tau}^{0} dz v(z+t) \right] \rangle = \int_{-\tau}^{0} dz K_{\xi v}(t'-z) e^{-R} .$$

Finally we can rewrite Eqs. (3.15), (3.16) as:

$$K_{\xi v}(t') = K_{\xi}(t') - a \int_0^{\infty} d\tau \sin \Omega\tau G(\tau) \int_{-\tau}^{0} dz K_{\xi v}(t'-z) e^{-R} , \tag{3.17}$$

$$K_{v}(t') = K_{\xi v}(-t') - a \int_0^{\infty} d\tau \sin \Omega\tau G(\tau) \int_{-\tau}^{0} dz K_{v}(t'-z) e^{-R} . \tag{3.18}$$

To proceed further it is convenient to consider the spectra $\mathcal{V}(w)$ in the following form:

$$\mathcal{V}(\omega) = \frac{1}{2\pi} \int_{-\infty}^{\infty} dt K_v(t) e^{-i\omega t} ,$$

and similarly for $\mathcal{S}$ and $\mathcal{C}$. Then Eqs. (3.17, 3.18) yield

$$\mathcal{S}(\omega) = \mathcal{C}(\omega) - a\mathcal{S}(\omega) \int_0^{\infty} d\tau \sin \Omega\tau G(\tau) e^{-R} \int_{-\tau}^{0} dz e^{-i\omega z} , \tag{3.19}$$

$$\mathcal{V}(\omega) = \mathcal{S}(-\omega) - a\mathcal{V}(\omega) \int_0^{\infty} d\tau \sin \Omega\tau G(\tau) e^{-R} \int_{-\tau}^{0} dz e^{-i\omega z} . \tag{3.20}$$

Equation (3.12) in the spectral form reads

$$R = \int_{-\infty}^{\infty} \frac{1 - \cos \omega\tau}{\omega^2} \mathcal{V}(\omega) d\omega . \tag{3.21}$$

Here we have used that $\mathcal{V}(\omega)$ is an even function. The integral (3.21) can be approximated as

$$R \approx \int_{-\infty}^{\infty} \frac{1 - \cos \omega\tau}{\omega^2} \mathcal{V}(0) d\omega = \frac{\tau D}{2} . \tag{3.22}$$

Substituting Eq. (3.22) in Eqs. (3.19,3.20) we obtain the final expressions for $\mathcal{S}(\omega)$ and $\mathcal{V}(\omega)$

$$\mathcal{S}(\omega) = \mathcal{C}(\omega) + a\frac{\mathcal{S}(\omega)}{i\omega} \int_0^{\infty} d\tau \sin \Omega\tau G(\tau) e^{-D\tau/2} (1 - e^{i\omega\tau}) , \tag{3.23}$$

$$\mathcal{V}(\omega) = \mathcal{S}(-\omega) + a\frac{\mathcal{V}(\omega)}{i\omega} \int_0^{\infty} d\tau \sin \Omega\tau G(\tau) e^{-D\tau/2} (1 - e^{i\omega\tau}) . \tag{3.24}$$

Excluding $\mathcal{S}(\omega)$ we get

$$\mathcal{V}(\omega) = \frac{\mathcal{C}(\omega)}{\left|1 - \dfrac{a}{i\omega}\int\limits_0^\infty d\tau \sin\Omega\tau G(\tau)e^{-D\tau/2}(1-e^{i\omega\tau})\right|^2} . \tag{3.25}$$

The diffusion constant D is related to the spectral density of the frequency fluctuations at zero frequency: $D = 2\pi\mathcal{V}(0)$. Thus, using Eq. (3.25) we obtain the equation for determination of the diffusion constant in the Gaussian approximation as

$$D = \frac{D_0}{\left[1 + a\int\limits_0^\infty d\tau\tau \sin\Omega\tau G(\tau)e^{-D\tau/2}\right]^2} , \tag{3.26}$$

where $D_0 = 2\pi\mathcal{C}(0)$ is the diffusion constant in the absence of the feedback.

3.2 Several particular cases

3.2.1 General proportional and proportional derivative feedback

In a more general case, the control term can be designed as a combination of the linear operators from x and $\dot{x}$, i.e.,

$$\begin{aligned}
\widehat{L}(x) = \widehat{L}_0(x) + \widehat{L}_1(\dot{x}) &= \int\limits_{-\infty}^{t} G_0(t-t')x(t')dt' + \int\limits_{-\infty}^{t} G_1(t-t')\dot{x}(t')dt' \\
&= \int\limits_{-\infty}^{t} G_0(t-t')x(t')dt' + G_1(0)x(t) + \int\limits_{-\infty}^{t} G_1'(t-t')x(t')dt' \\
&= \int\limits_{-\infty}^{t} \Big[G_0(t-t') + 2G_1(0)\delta(t-t') + G_1'(t-t')\Big]x(t')dt' \\
= \int\limits_0^\tau \Big[G_0(\tau) + 2G_1(0)\delta(\tau) + G_1'(\tau)\Big]x(t-\tau)d\tau &= \int\limits_0^\tau G(\tau)x(t-\tau)d\tau ,
\end{aligned} \tag{3.27}$$

where $G(\tau) = G_0(\tau) + 2G_1(0)\delta(\tau) + G_1'(\tau)$, and can be used for computation of the phase diffusion constant by virtue of formulas obtained above.

3.2.2 Controlling oscillator coherence by a linear damped oscillator

As an example of a feedback loop we take the damped harmonic oscillator,

$$\ddot{u} + \alpha\dot{u} + \omega_0^2 u = x \ . \tag{3.28}$$

The Green's function for the damped harmonic oscillator is given by:

$$G(\tau)_{osc} = \frac{1}{y_1 - y_2}(e^{y_1\tau} - e^{y_2\tau}) \ , \tag{3.29}$$

where $y_{1,2}$ are the roots of quadratic equation

$$y^2 + \alpha y + w_0^2 = 0 \ .$$

Substituting $y_{1,2} = -\alpha/2 \pm \sqrt{\alpha^2/4 - \omega_0^2} = -\alpha/2 \pm i\omega_0'$ into the expression for the Green function (3.29) we obtain

$$G(\tau)_{osc} = \frac{1}{2i\omega_0'}[e^{-\alpha\tau/2}(e^{i\omega_0'\tau} - e^{-i\omega_0'\tau})] = \frac{e^{-\alpha\tau/2}\sin\omega_0'\tau}{\omega_0'} \ . \tag{3.30}$$

Below we consider the particular case, namely, controll of oscillator coherence by the *proportional derivative control*.

3.2.3 Proportional derivative control

Let us consider proportional derivative control, which is designed as

$$\widehat{L}(x) \ = \ \widehat{L}_1(x) = \int\limits_{-\infty}^{t} G_1(t-t')\dot{x}(t')dt' = \int\limits_{0}^{\tau}\Big[2G_1(0)\delta(\tau) + G_1'(\tau)\Big]x(t-\tau)d\tau = \int\limits_{0}^{\tau} G(\tau)x(t-\tau)d\tau \ , \tag{3.31}$$

where

$$G(\tau) = 2G_1(0)\delta(\tau) + G_1'(\tau) = e^{-\alpha\tau/2}(\cos\omega_0'\tau - \frac{\alpha}{2\omega_0'}\sin\omega_0'\tau) \ . \tag{3.32}$$

Substituting (3.32) in the Eq. (3.6) leads to equation for the frequency Ω,

$$\Omega - a\int\limits_{0}^{\infty}\Big[2G_1(0)\delta(\tau) + G_1'(\tau)\Big]\cos\Omega\tau d\tau = \Omega_0 \ ,$$

$$\Omega - a\Omega \int_0^\infty G_{osc}(\tau) \sin \Omega\tau d\tau = \Omega_0 \ .$$

Thus, the equation for the oscillation frequency in the *linear approximation* can be read as

$$\Omega - \frac{a\Omega}{\omega_0'} \int_0^\infty e^{-\alpha\tau/2} \sin \omega_0'\tau \sin \Omega\tau d\tau = \Omega_0 \ .$$

Substituting (3.32) in the Eq. (3.8) we get the expression for the diffusion constant in the *linear approximation*

$$D = \frac{D_0}{\left[1 + a \int_0^\infty e^{-\alpha\tau/2}(\cos \omega_0'\tau - \frac{\alpha}{2\omega_0'} \sin \omega_0'\tau)\tau \sin \Omega\tau d\tau\right]^2} \ . \tag{3.33}$$

Substituting (3.32) in the Eqs. (3.11), (3.26) we get the equations for the frequency and the diffusion constant in the *Gaussian approximation,* correspondingly,

$$\Omega - a \int_0^\infty e^{-(\alpha+D)\tau/2}(\cos \omega_0'\tau - \frac{\alpha}{2\omega_0'} \sin \omega_0'\tau) \cos \Omega\tau d\tau = \Omega_0 \ ,$$

$$D = \frac{D_0}{\left[1 + a \int_0^\infty e^{-(\alpha+D)\tau/2}(\cos \omega_0'\tau - \frac{\alpha}{2\omega_0'} \sin \omega_0'\tau)\tau \sin \Omega\tau d\tau\right]^2} \ . \tag{3.34}$$

Finally, we obtain the main results of our analysis — closed system of two equations in the *linear approximation*

$$\Omega - \frac{16a\alpha\Omega^2}{\big((\Omega+\omega)^2 + \alpha^2/4\big)\big((\Omega-\omega)^2 + \alpha^2/4\big)} = \Omega_0 \ ,$$

$$D = \frac{D_0}{\left[1 + \dfrac{2a\alpha\Omega\big(\Omega^4 - (\omega^2 + \alpha^2/4)^2\big)}{\big((\Omega+\omega)^2 + \alpha^2/4\big)^2\big((\Omega-\omega)^2 + \alpha^2/4\big)^2}\right]^2} \ , \tag{3.35}$$

and in the *Gaussian approximation*

$$\Omega + \frac{16a\alpha\Omega^2 + 2aD\big((\alpha+D)^2 + 4(\Omega^2+\omega^2)\big)}{\Big((\Omega+\omega)^2 + \dfrac{(\alpha+D)^2}{4}\Big)\Big((\Omega-\omega)^2 + \dfrac{(\alpha+D)^2}{4}\Big)} = \Omega_0 \ , \tag{3.36}$$

$$
\begin{aligned}
D &= D_0 \Big/ \Big[1 + (16\Omega a D^5 + 32\Omega a\alpha D^4 - 32\Omega a(\alpha^2 + 4\omega^2 - 4\Omega^2)D^3 \\
&\quad +128\Omega a\alpha(-2\omega^2 - \alpha^3 + 2\Omega^2)D^2 + 16\Omega a(-7\alpha^4 - 48\omega^4 + 8\Omega^2\alpha^2 + 16\Omega^4 \\
&\quad +32\Omega^2\omega^2 - 40\omega^2\alpha^2)D - 512\Omega a\omega^4\alpha + 512\Omega^5 a\alpha - 256\Omega a\omega_0'^2\alpha^3 - 32\Omega a\alpha^5) \\
&\quad \times\big((\Omega + \omega_0')^2 + (\alpha + D)^2/4\big)^{-2}\big((\Omega - \omega_0')^2 + (\alpha + D)^2/4\big)^{-2}\Big]^2 . \qquad (3.37)
\end{aligned}
$$

These systems for two variables D and Ω have been solved numerically and the results are presented in Figs. 3.1, 3.2, 3.3. First we analyze the dependence of the diffusion constant D on the the oscillatordamping factor α (3.39). It is seen that the feedback control essentially changes the diffusion constant for small values of α. With an increase of the band pass of the filter the control effect almost vanishes (see Fig. 3.3).

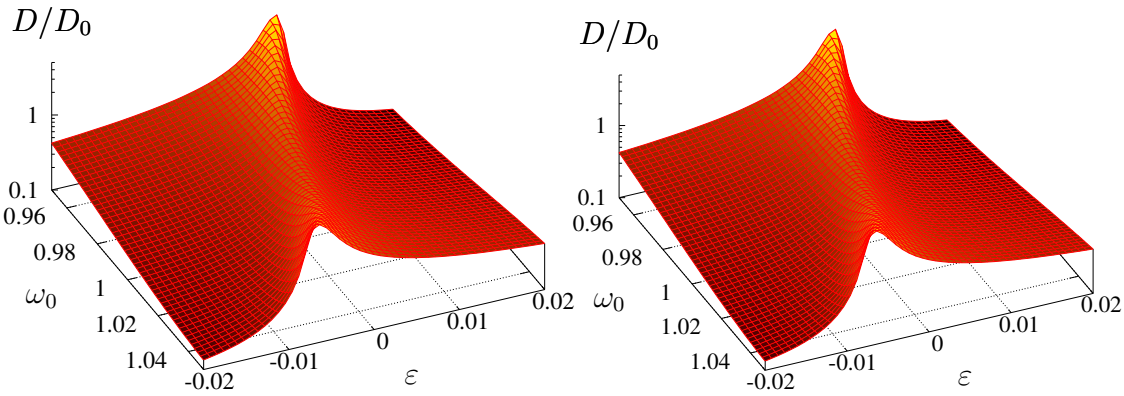

Figure 3.1: Diffusion constant D for the phase of the controlled noise driven Van der Pol oscillator as the function of oscillator frequency ω_0 and ε in linear (left panel) and Gaussian (right panel) approximation for $\alpha = 0.08\omega_0$ and $D_0 = 0.0024$.

Next, we analyze the impact of the oscillator frequency ω_0. From Figs. 3.1,3.2, 3.3 one can see that there is only a slight difference between these two approximations. This difference is more noticeable in Fig. 3.4, where we show the analytical results of linear (a) and Gaussian (b) approximations of diffusion constant D for different values of oscillator frequency.

Below we compare numerical solutions of the analytically obtained equations with direct numerical simulations.

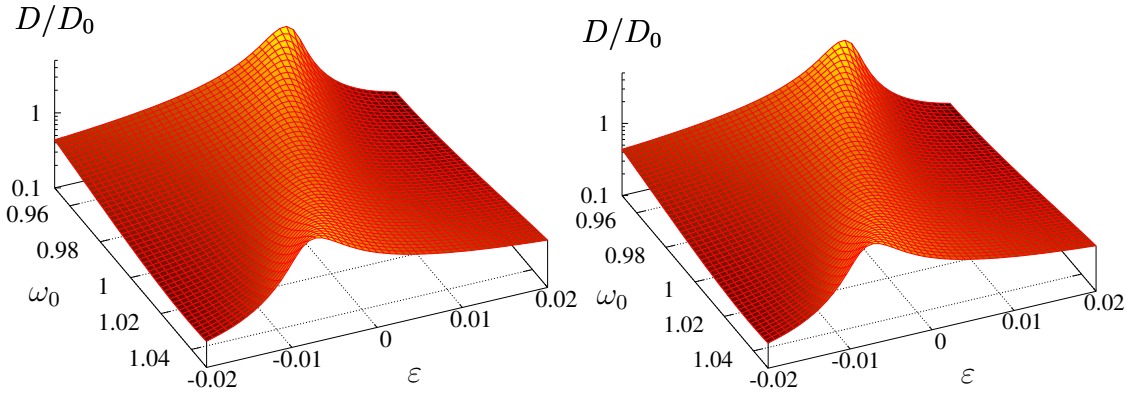

Figure 3.2: Diffusion constant D for the phase of the controlled noise driven Van der Pol oscillator as the function of oscillator frequency ω_0 and ε in linear (right panel) and Gaussian (right panel) approximation for $\alpha = 0.1\omega_0$ and $D_0 = 0.0024$.

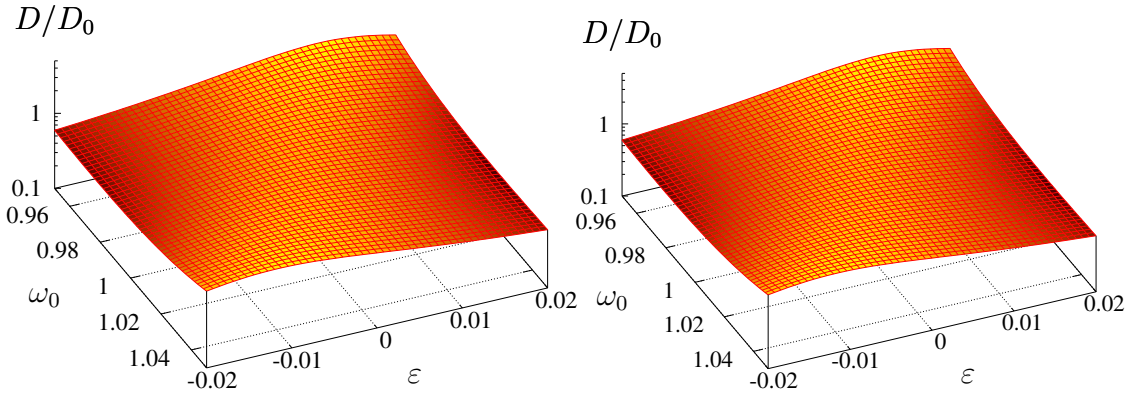

Figure 3.3: Diffusion constant D for the phase of the controlled noise driven Van der Pol oscillator as the function of oscillator frequency ω_0 and ε in linear (left panel) and Gaussian (right panel) approximation for $\alpha = 0.2\omega_0$ and $D_0 = 0.0024$.

3.3 Numerical results

In this section we verify the above derived theory by the results of numerical simulation of a noisy Van der Pol oscillator. As a passive system we take a linear damped oscillator and the control signal which is fed back into the system has the form $\widehat{L}(x) = \dot{u}$.

$$\ddot{x} \quad - \quad \mu(1-x^2)\dot{x} + \Omega_0 x = \varepsilon\dot{u} + \zeta(t)\ , \quad \langle\zeta(t)\zeta(t')\rangle = 2d^2\delta(t-t')\ , \tag{3.38}$$

$$\ddot{u} \quad + \quad \alpha\dot{u} + \omega_0^2 u = x\ . \tag{3.39}$$

In the presence of control the diffusion can be suppressed or enhanced de-

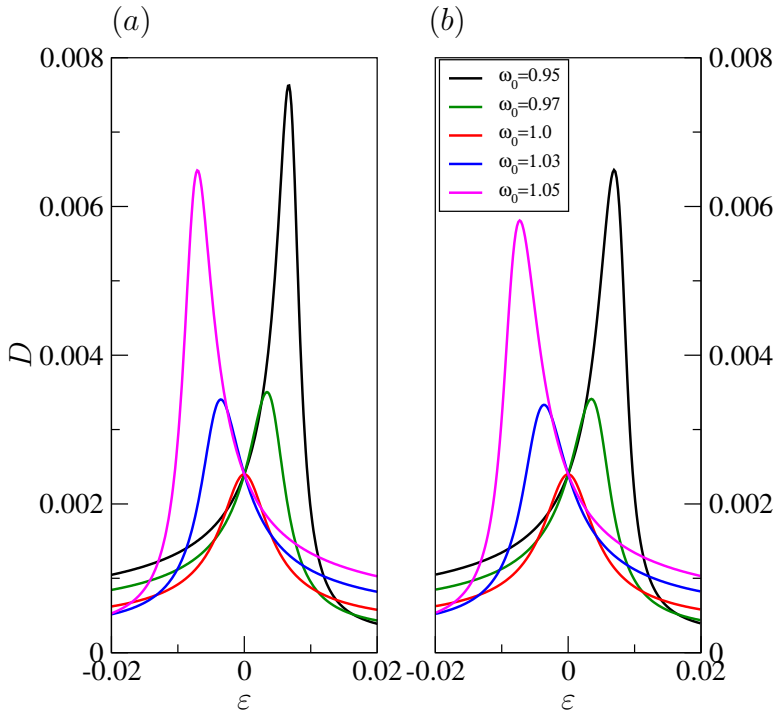

Figure 3.4: Theoretical results of linear (a) and Gaussian (b) approximations of diffusion constant D for different values of oscillator frequency and for $\alpha = 0.1\omega_0$.

pending on the feedback strength ε, which is confirmed by the numerical results in Fig. 3.5 (blue curve) for $\Omega_0 = \omega_0 = 1$, $\alpha = 0.1\omega_0$, $d = 0.1$, and $\mu = 0.2$. Black and red curves correspond to theoretical results for linear (Eq. (3.35)) and Gaussian (Eq. (3.37)) approximations, respectively, for the following set of parameters: $\Omega_0 = \omega_0 = 1.0$, $\alpha = 0.1\omega_0$, $D_0 = 0.0024$. The correspondence between the numerics and analytical results is very good in the case of small values of the feedback strength ε.

In Fig. 3.6 we plot the diffusion constant D as a function of ε of controlled Van der Pol model for different values of oscillator frequency ω_0. Depending on ω_0 on can see that the curves are shifted with respect to the curve for $\omega_0 = 1.0$.

We point out that, although we derived the theory for the van der Pol equation, a similar phase equation (3.4) can be obtained for any limit cycle oscillator. As the phase dynamics of some chaotic oscillators is qualitatively similar to the dynamics of noisy periodic oscillators (see Ref. (64)), Eq. (3.4) can also be used for chaotic oscillators in the presence of the feedback loop.

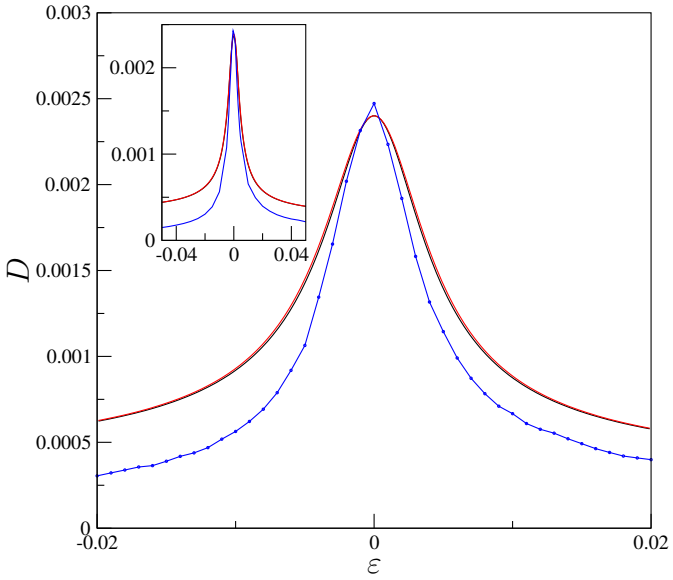

Figure 3.5: The dependence of the phase diffusion constant D on the feedback strength ε for the controlled Van der Pol model. The control is implemented by linear passive oscillator Eq. (3.39). Blue curve represents results of numerical simulation (Eqs. (3.38), (3.39)); black and red curves represent theoretical results of linear Eq. (3.35) and Gaussian Eq. (3.37) approximations, respectively.

To prove it numerically we consider the chaotic Lorenz system, controlled by the passive oscillator (3.39)

$$\begin{aligned} \dot{x} &= \sigma(y-x)\,, \\ \dot{y} &= rx - y - xz\,, \\ \dot{z} &= -bz + xy + \varepsilon\dot{u}\,, \\ \ddot{u} &+ \alpha\dot{u} + \omega_0^2 u = z\,, \end{aligned} \tag{3.40}$$

where $\sigma = 10$, $r = 28$, and $b = 8/3$. The phase of the Lorenz system is well-defined if one uses a projection of the phase space on the plane $(u = \sqrt{x^2+y^2}, z)$ (see (64) and Fig. 3.9 below):

$$\phi = \arctan\frac{z(t)-z_0}{y(t)-u_0}\,,$$

where the point $\{u_0 = 2b(r-1), z_0 = r-1\}$ corresponds to the nontrivial fixed points of the Lorenz system. Notice that there is no noise term in Eqs. (3.40).

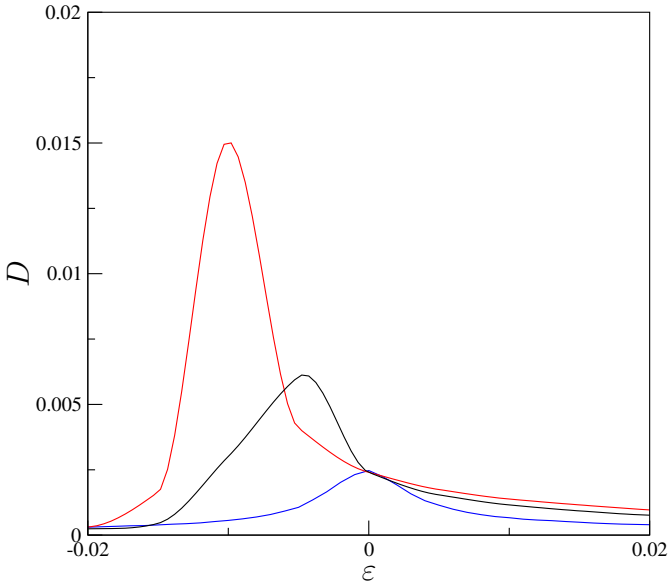

Figure 3.6: Results of numerical simulation for the controlled Van der Pol model (3.38), (3.39) for different values of the oscillator frequency: $\omega_0 = 1.0$ (blue curve), $\omega_0 = 1.05$ (black curve), $\omega_0 = 1.07$ (red curve).

However, due to chaos, the phase of the autonomous system grows non-uniformly, with a non-zero diffusion constant. The diffusion constant D as the function of the feedback strength ε is shown in Fig. (3.7). The diffusion constant strongly depends on the frequency ω_0 of the linear damped oscillator, which play the role of the band pass filter. This dependence for Lorenz system is demonstrated in Fig. 3.8.

It is noteworthy, that the effect of suppression of diffusion in not due to the suppression of the chaos. It is seen from Fig. 3.9, where we show the projections of the phase portrait for the system without feedback and also for maximal suppression and enhancement.

Another way to represent the effect of the linear oscillator on the coherence can be also given by the power spectrum. The power spectrum has a peak at frequency Ω_0, and the width of the peak is proportional to the diffusion constant D. It is seen from Fig. 3.10 that the feedback control in the case of suppression of the diffusion makes the spectral peak essentially more narrow (a) and vice versa, more wide in the case of enhancement (b).

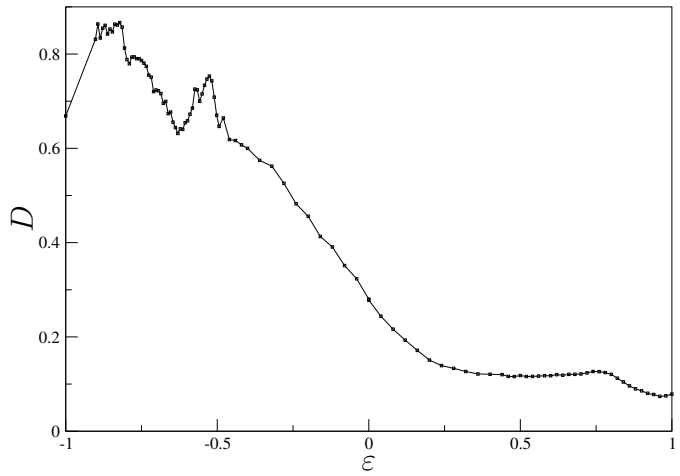

Figure 3.7: Diffusion constant D for the phase of the controlled Lorenz system (3.40) as the function of feedback strength ε, for $\omega_0 = 2\pi/0.76$, $\alpha = 0.1\omega_0$.

3.4 Summary and discussion

In this chapter we have demonstrated that linear feedback is an effective tool to control coherence of noisy limit cycle oscillators, as well as of chaotic systems, where the computation of the phase is possible. Using the Gaussian approximation, we have derived a system of equations for the diffusion constant and the mean frequency. The numerical calculations show that this theory works pretty good if the feedback is not very strong. The situation in the case of strong feedback, where several stable oscillation frequencies are possible, remains unsolved and will be considered elsewhere.

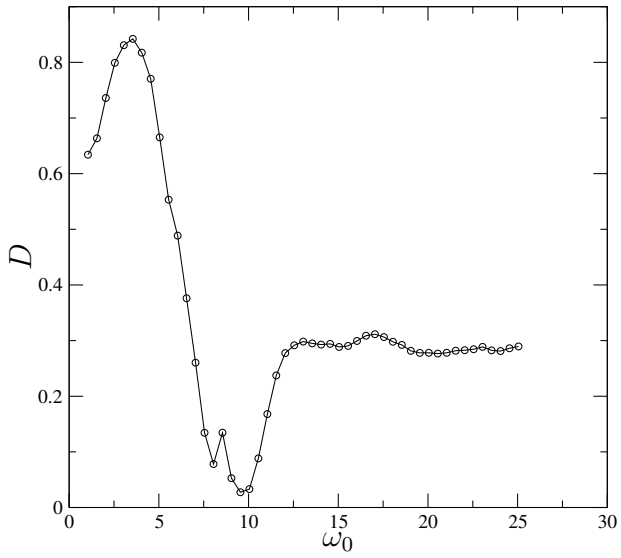

Figure 3.8: The dependence of the diffusion constant D for the phase of the controlled Lorenz system (3.40) on the oscillator frequency ω_0, for $\varepsilon = 0.5$, $\alpha = 0.1\omega_0$.

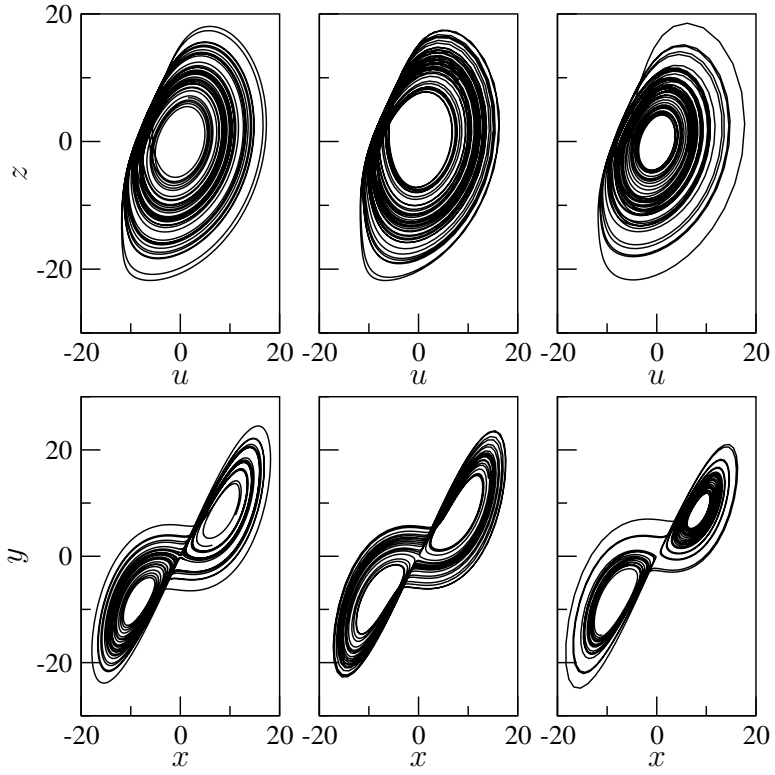

Figure 3.9: The projections of the phase portrait for the Lorenz system (3.40) in the absence of feedback, $D = 0.28$ (left column) and in the presence of feedback for $\varepsilon = 0.96$, $D = 0.08$ (middle column), $\varepsilon = -0.88$, $D = 0.85$ (right column). Parameters are: $\omega_0 = 2\pi/0.76$, $\alpha = 0.1\omega_0$.

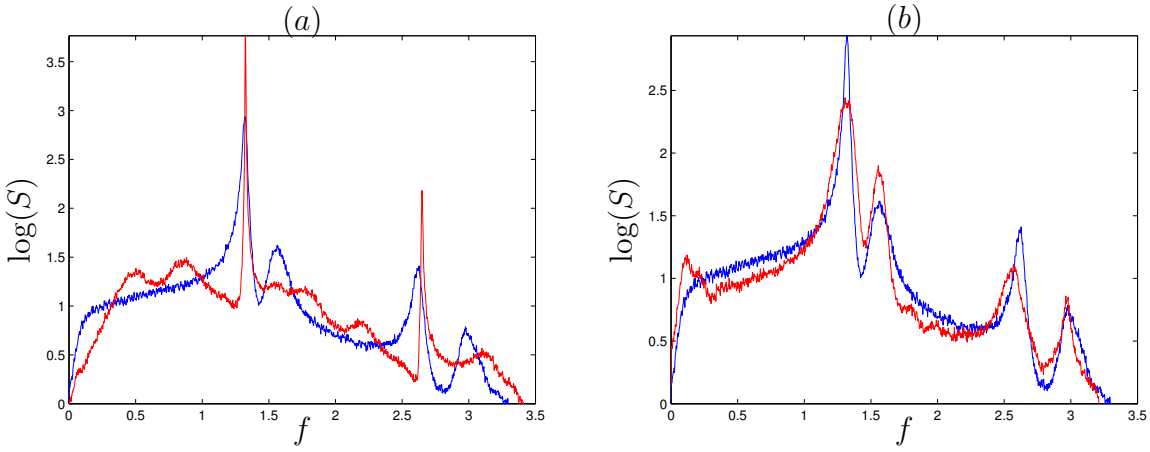

Figure 3.10: Spectra $S(f)$ of the z component of the Lorenz system (3.40) for $\varepsilon = 0.5$ (a) and for $\varepsilon = -0.3$ (b). The red curve corresponds to the controlled Lorenz system, whereas the blue curve corresponds to the system without control. Other parameters: $\omega_0 = 2\pi/0.76$, $\alpha = 0.1\omega_0$.

Chapter 4

Conclusion

In the present doctoral study we have discussed the control problem of systems as diverse as stochastic limit cycles, deterministic chaotic oscillators and neural ensembles. Particularly, a technique which ensures an efficient control of such diverse systems has been developed. The main concept of this thesis is to relate nonlinear dynamics with control theory for the purpose of control of complex systems. From the viewpoint of control theory, our suggested approach is an extension of filter-based techniques (54; 49), where a filter in the feedback loop estimates the fixed point dynamically and eventually stabilizes it. From the viewpoint of nonlinear dynamics, our method dates back to the classical problem of the oscillation theory, viz. to the problem of interaction of an active oscillator (or medium) with a passive one. It is known that for certain parameter values the load can quench the active system. In our approach we exploit this idea in order to control such diverse complex dynamical systems as a neural population and a noisy or chaotic self-sustained oscillatory system.

In the following, we discuss the main results of the work and open questions. We have started with the application of the suggested technique to an isolated population of neurons with a purpose to suppress the collective synchrony. This problem is motivated by a hypothesis that for neurolagical diseases like Parkinsons, symptoms result from a synchronized pacemaker-like activity of a population of many thousands of neurons in the basal ganglia, whereas a normal functioning of the basal ganglia is characterized by an uncorrelated firing of neurons. This hypothesis is supported by several experimental stud-

ies (43; 44; 45; 46). Having in mind possible application in neuroscience, our main requirement to the suppresion technique is to provide control with vanishing stimulation and thus minimizing invasion into the system. We have shown, that this can be achieved by a specialy designed feedback loop with a built-in second-order filter. We have supported our idea by numerical simulation of the ensemble dynamics using the idealized model of globally coupled neurons. We have also modelled a more realistic neuronal ensemble with all-to-all synaptic connections and numerical analysis also indicates that our approach works in this case as well. Furthermore, we extended our feedback approach for control of synchrony to a more complex setting of two interacting populations, where the first one is affected by stimulation, whereas measurement is performed from the second one. The considered situation can model suppression of pathological rhythm when registration and stimulation of the brain tissue cannot be carried out by the same or closely placed electrode(s). We have considered the cases when the second population is either active or passive; the latter case may describe measurements by a surface electrode. The theoretical analysis of suppression can be performed in the framework of the model amplitude equation and the results are in a good agreement with simulations.

Important advantages of our *linear feedback* control are simplicity of its implementation, an ability to compensate a phase shift inherent to stimulation as well as a latency in measurements, and presence of a built-in bandpass filter. The last one allows one to extract the relevant signal from its mixture with other rhythms and noise; the central frequency and the bandwidth of the filter are governed by parameters ω_0 and α. With this method we also overcome the main disadvantage of the time-delayed method, namely a new instability can arise if the delay is large enough. The parameters of the control scheme can be easily tuned by means of a test stimulation by a harmonic force. We expect that our technique can contribute significantly to the development of mild and efficient techniques for suppression of pathological brain activity. The main advantage of the suggested technique is that the administered control input vanishes as soon as a desynchronized state is achieved. This feature is extremely important for therapeutic applications, since it means significant reduction of intervention into a living tissue. As a problem for ongoing research we mention a development of

an adaptive, self-tuning suppression technique.

Next, we have demonstrated the effect of the coherence control by means of a *linear feedback*. The control is possible for noisy limit cycles oscillators as well as for chaotic systems. The coherence, or constancy of oscillation frequency, is a crucial property of the dynamics determining their quality as clocks. As a characteristic of coherence we have used the phase diffusion constant, which is proportional to the width of the spectral peak of oscillations. We have developed a statistical theory of phase diffusion under the influence of a general *linear feedback* and validated it by numerical results. Using the Gaussian approximation, we have derived a closed system of equations for the diffusion constant and the mean frequency. The theory works if the feedback is not very strong, or if the noise is strong enough to suppress multistability in mean frequency. The case of multistability gives some opportunities for possible direction of the future development.

The suggested technique may possibly substitute delayed-feedback schemes in some other applications, e.g., in stabilization of low-dimensional systems (13; 50; 51; 52; 54; 55; 49; 53; 12), control of noise-induced oscillations (66), etc.

Appendices

Appendix A

Stability domain of the model equation

Computation of the determinant of system (2.7) provides

$$\lambda^5\mu + \lambda^4(1+\alpha\mu-2\xi\mu) + \lambda^3(\xi^2\mu - \mathcal{E}\mu\cos\beta + 2\omega^2\mu - 2\xi\alpha\mu + \alpha - 2\xi)$$
$$+\lambda^2(\omega^2\alpha\mu - \mathcal{E}\cos\beta - \mathcal{E}\gamma\cos\beta - 2\xi\omega^2\mu - 2\xi\alpha + \xi\mathcal{E}\mu\cos\beta + \xi^2\alpha\mu + \omega\mathcal{E}\mu\sin\beta + 2\omega^2 + \xi^2)$$
$$+\lambda(\omega\mathcal{E}\sin\beta + \xi\mathcal{E}\cos\beta + \omega\mathcal{E}\gamma\sin\beta + \xi^2\omega^2\mu + \omega^4\mu + \omega^2\alpha + \xi^2\alpha - 2\xi\omega^2 + \xi\mathcal{E}\gamma\cos\beta)$$
$$+\xi^2\omega^2 + \omega^4 = 0\,. \quad \text{(A.1)}$$

Stability domain in the parameter plane $(\gamma, \mathcal{E})$, or, equivalently in the parameter plane (θ, ε_f), is determined by the condition $\mathrm{Re}(\lambda) < 0$. (We remind that $\gamma = -\omega\mu\tan\theta$ and $\mathcal{E} = \varepsilon_f\cos\theta$.) Taking $\lambda = i\Omega$ on the stability border and separating real and imaginary parts, we obtain

$$\Omega^4(\alpha\mu + 1 - 2\xi\mu) + \Omega^2[\mathcal{E}\cos\beta(1 - \xi\mu + \gamma) - \omega\mu\mathcal{E}\sin\beta + 2\xi\alpha - 2\omega^2 - \xi^2 + 2\xi\omega^2\mu - \omega^2\alpha\mu$$
$$-\xi^2\alpha\mu] + \omega^4 + \xi^2\omega^2 = 0\,, \quad \text{(A.2)}$$

$$\Omega\{\Omega^4\mu + \Omega^2[\mu(\mathcal{E}\cos\beta - \xi^2 - 2\omega^2 + 2\xi\alpha) + 2\xi - \alpha] + \mathcal{E}(1+\gamma)(\omega\sin\beta + \xi\cos\beta)$$
$$+\omega^2(\xi^2\mu + \alpha - 2\xi) + \omega^4\mu + \xi^2\alpha\} = 0\,. \quad \text{(A.3)}$$

Thus, we have two equations for two variables $(\gamma, \mathcal{E})$, and Ω is a parameter. It is easy to check that $\Omega = 0$ provides no solution, therefore we divide the Eq. (A.3)

by $\Omega \neq 0$ and express $\mathcal{E}$ from this equation. Substituting it into the Eq. (A.2) we get γ. Then, substituting γ into the expression for $\mathcal{E}$ we finally obtain $\mathcal{E}$. Hence,

$$\gamma = A/B \ ,$$

where

$$A = \omega \sin\beta[\Omega^6\mu^2 + \Omega^4(1 - 2\omega^2\mu^2 + 2\mu^2\xi\alpha - \mu^2\xi^2) + \Omega^2(\omega^2\mu^2\xi^2 - 2\omega^2 + \omega^4\mu^2 + 2\xi\alpha - \xi^2) + \xi^2\omega^2 + \omega^4] + \cos\beta[\Omega^6(\alpha\mu^2 - \xi\mu^2) + \Omega^4(\alpha - \xi - \xi^3\mu^2 + \xi^2\mu^2\alpha - \omega^2\alpha\mu^2) + \Omega^2(\xi^2\alpha - \omega^2\alpha - \xi^3 + \xi\mu^2\omega^4 + \xi^3\mu^2\omega^2) + \xi^3\omega^2 + \omega^4\xi] \ , \quad \text{(A.4)}$$

$$B = \omega \sin\beta[\Omega^4(2\xi\mu - \alpha\mu - 1) + \Omega^2(\xi^2\alpha\mu - 2\xi\omega^2\mu - 2\xi\alpha + \xi^2 + \omega^2 + \omega^2\alpha\mu) - \xi^2\omega^2 - \omega^4] + \cos\beta[\Omega^6\mu + \Omega^4(\alpha\mu\xi + \xi^2\mu - 2\omega^2\mu + \xi - \alpha) + \Omega^2(\omega^4\mu - \xi^2\omega^2\mu + \omega^2\alpha\mu\xi + \xi^3\alpha\mu - \xi^2\alpha + \omega^2\alpha + \xi^3) - \xi^3\omega^2 - \omega^4\xi] \ . \quad \text{(A.5)}$$

and

$$\mathcal{E} = C/D \ ,$$

where

$$C = \cos\beta[-\Omega^6\mu + \Omega^4(2\omega^2\mu - \xi^2\mu - \alpha\mu\xi + \alpha - \xi) + \Omega^2(\xi^2\omega^2\mu - \xi^3 - \omega^4\mu - \xi^3\alpha\mu - \omega^2\alpha\mu\xi + \xi^2\alpha - \omega^2\alpha) + \xi^3\omega^2 + \omega^4\xi] + \omega \sin\beta[\Omega^4(1 - 2\xi\mu + \alpha\mu) + \Omega^2(2\xi\alpha + 2\xi\omega^2\mu - \omega^2\alpha\mu - \xi^2\alpha\mu - \xi^2 - 2\omega^2) + \omega^4 + \xi^2\omega^2] \ , \quad \text{(A.6)}$$

$$D = \mu\Omega^2[\xi\omega \sin 2\beta + \omega^2 + \cos^2\beta(\Omega^2 + \xi^2 - \omega^2)] \ . \quad \text{(A.7)}$$

Appendix B

Maple code for stability analysis of the model equation (2.13)

```
> with(LinearAlgebra):
> M:=Matrix(7,[[lambda-xi1+epsilon,omega1,-epsilon,0,0,-k*cos(beta),
-gmk*cos(beta)],[-omega1,lambda-xi1+epsilon,0,-epsilon,0,-k*sin(beta),
-gmk*sin(beta)],[-epsilon,0,lambda-xi2+epsilon,omega2,0,0,0],[0,
-epsilon,-omega2,lambda-xi2+epsilon,0,0,0],[0,0,0,0,lambda,-1,0],
[0,0,-1,0,omega^2, lambda+alpha,0],[0,0,0,0,-lambda,0,mu*lambda+1]]);

  M :=

        [lambda - xi1 + epsilon , omega1 , -epsilon , 0 , 0 ,

        -k cos(beta) , -gmk cos(beta)]

        [-omega1 , lambda - xi1 + epsilon , 0 , -epsilon , 0 ,

        -k sin(beta) , -gmk sin(beta)]

        [-epsilon , 0 , lambda - xi2 + epsilon , omega2 , 0 , 0 , 0]

        [0 , -epsilon , -omega2 , lambda - xi2 + epsilon , 0 , 0 , 0]

        [0 , 0 , 0 , 0 , lambda , -1 , 0]

        [                     2                    ]
```

```
        [0 , 0 , -1 , 0 , omega  , lambda + alpha , 0]

        [0 , 0 , 0 , 0 , -lambda , 0 , mu lambda + 1]

> det:=Determinant(M):
> collect(det, lambda^7):
> eq:=subs(lambda=I*Omega, det):
> eqtmp:=evalc(eq):
> eqr:=omega1^2*Omega^4-Omega^6*alpha*mu+Omega^4*omega^2
+xi2^2*Omega^4+xi1^2*Omega^4-Omega^6+xi1^2*xi2^2*omega^2
+xi1^2*epsilon^2*omega^2+xi1^2*omega2^2*omega^2
+epsilon^2*xi2^2*omega^2+epsilon^2*omega2^2*omega^2
-2*xi1^2*xi2*epsilon*omega^2+omega1^2*xi2^2*omega^2
+omega1^2*epsilon^2*omega^2+omega1^2*omega2^2*omega^2
+2*xi1*xi2*epsilon^2*omega^2-2*xi1*epsilon*xi2^2*omega^2
-2*xi1*epsilon*omega2^2*omega^2-2*omega1^2*xi2*epsilon*omega^2
+2*omega1*epsilon^2*omega2*omega^2-4*Omega^6*epsilon*mu
+2*Omega^6*xi2*mu-2*Omega^4*xi2*alpha+4*Omega^4*epsilon*alpha
-6*xi2*epsilon*Omega^4-2*xi1*Omega^4*alpha+4*xi1*Omega^4*xi2
-6*xi1*Omega^4*epsilon+4*xi2*epsilon^2*Omega^2*alpha
+6*Omega^2*xi2*epsilon*omega^2-4*xi1*Omega^2*xi2*omega^2
-2*Omega^4*xi2*omega^2*mu+4*Omega^4*epsilon*omega^2*mu
+xi2^2*alpha*mu*Omega^4+4*epsilon^2*alpha*mu*Omega^4
+omega2^2*alpha*mu*Omega^4-Omega^2*xi2^2*omega^2
-4*Omega^2*epsilon^2*omega^2-Omega^2*omega2^2*omega^2
+2*xi1*Omega^6*mu-xi1^2*Omega^2*omega^2-xi1^2*omega2^2*Omega^2
-xi1^2*epsilon^2*Omega^2-xi1^2*xi2^2*Omega^2
-epsilon^2*xi2^2*Omega^2-epsilon^2*omega2^2*Omega^2
+4*epsilon^2*Omega^4+omega2^2*Omega^4-omega1^2*epsilon^2*Omega^2
-omega1^2*Omega^2*omega^2+2*omega1^2*Omega^2*xi2*omega^2*mu
-2*omega1^2*Omega^2*epsilon*omega^2*mu
-omega1^2*xi2^2*alpha*mu*Omega^2-omega1^2*epsilon^2*alpha*mu*Omega^2
-4*xi2*epsilon^2*mu*Omega^4-2*xi1*Omega^4*omega^2*mu
+6*xi1*Omega^2*epsilon*omega^2+2*xi1*xi2^2*Omega^2*alpha
+4*xi1*epsilon^2*Omega^2*alpha+2*xi1*omega2^2*Omega^2*alpha
-2*epsilon*xi2^2*Omega^2*alpha-2*epsilon*omega2^2*Omega^2*alpha
+2*xi1^2*Omega^2*xi2*alpha-2*xi1^2*Omega^2*epsilon*alpha
+2*xi1^2*xi2*epsilon*Omega^2-2*xi1*xi2*epsilon^2*Omega^2
+2*xi1*epsilon*xi2^2*Omega^2+2*xi1*epsilon*omega2^2*Omega^2
+2*omega1^2*Omega^2*xi2*alpha-2*omega1^2*Omega^2*epsilon*alpha
```

```
+2*omega1^2*xi2*epsilon*Omega^2-2*omega1*epsilon^2*omega2*Omega^2
-2*xi1*xi2^2*mu*Omega^4-4*xi1*epsilon^2*mu*Omega^4
-2*xi1*omega2^2*mu*Omega^4+2*epsilon*xi2^2*mu*Omega^4
+2*epsilon*omega2^2*mu*Omega^4+xi1^2*Omega^4*alpha*mu
-2*xi1^2*Omega^4*xi2*mu+2*xi1^2*Omega^4*epsilon*mu
-6*xi2*epsilon*alpha*mu*Omega^4+4*xi2*epsilon^2*omega^2*mu*Omega^2
+4*xi1*Omega^4*xi2*alpha*mu-6*xi1*Omega^4*epsilon*alpha*mu
+2*xi1*xi2^2*omega^2*mu*Omega^2+8*xi1*xi2*epsilon*mu*Omega^4
-8*xi1*xi2*epsilon*Omega^2*alpha+4*xi1*epsilon^2*omega^2*mu*Omega^2
+2*xi1*omega2^2*omega^2*mu*Omega^2-8*xi1*xi2*epsilon*omega^2*mu*Omega^2
-2*epsilon*xi2^2*omega^2*mu*Omega^2
-2*epsilon*omega2^2*omega^2*mu*Omega^2+2*xi1^2*Omega^2*xi2*omega^2*mu
-2*xi1^2*Omega^2*epsilon*omega^2*mu-xi1^2*xi2^2*alpha*mu*Omega^2
-xi1^2*epsilon^2*alpha*mu*Omega^2-xi1^2*omega2^2*alpha*mu*Omega^2
+2*xi1^2*xi2*epsilon*alpha*mu*Omega^2-epsilon^2*xi2^2*alpha*mu*Omega^2
-epsilon^2*omega2^2*alpha*mu*Omega^2-omega1^2*xi2^2*Omega^2
-omega1^2*omega2^2*Omega^2+omega1^2*Omega^4*alpha*mu
-2*omega1^2*Omega^4*xi2*mu+2*omega1^2*Omega^4*epsilon*mu
+2*epsilon^2*Omega^2*k*cos(beta)-2*xi1*xi2*epsilon^2*alpha*mu*Omega^2
+2*xi1*epsilon*xi2^2*alpha*mu*Omega^2+2*xi1*epsilon*omega2^2*alpha*mu*Omega^2
-omega1^2*omega2^2*alpha*mu*Omega^2+2*omega1^2*xi2*epsilon*alpha*mu*Omega^2
-2*omega1*epsilon^2*omega2*alpha*mu*Omega^2-epsilon*omega2*Omega^2*k*sin(beta)
-epsilon*omega2*Omega^2*k*gm*sin(beta)-epsilon^2*omega2*Omega^2*k*sin(beta)*mu
+xi1*epsilon*omega2*Omega^2*k*sin(beta)*mu
-omega1*epsilon*omega2*Omega^2*k*cos(beta)*mu
-omega1*epsilon^2*Omega^2*k*sin(beta)*mu+2*epsilon^2*Omega^2*gm*k*cos(beta)
-xi1*epsilon^2*Omega^2*k*cos(beta)*mu-epsilon^2*xi2*Omega^2*k*cos(beta)*mu
-epsilon*omega1*Omega^2*k*sin(beta)-epsilon*Omega^4*k*cos(beta)*mu
-epsilon*xi2*Omega^2*k*cos(beta)-epsilon*xi1*Omega^2*k*cos(beta)
-epsilon*omega1*Omega^2*k*gm*sin(beta)
+epsilon*omega1*xi2*Omega^2*k*sin(beta)*mu-epsilon*xi2*Omega^2*gm*k*cos(beta)
-epsilon*xi1*Omega^2*gm*k*cos(beta)+epsilon*xi1*xi2*Omega^2*k*cos(beta)*mu:

> eqm:=-omega1^2*Omega^3*alpha+2*xi1*Omega^3*omega^2+2*xi1*omega2^2*Omega^3
+4*xi1*epsilon^2*Omega^3+Omega^5*omega^2*mu+2*Omega^3*xi2*omega^2
-4*Omega^3*epsilon*omega^2+xi2^2*mu*Omega^5-xi2^2*Omega^3*alpha
+4*epsilon^2*mu*Omega^5-4*epsilon^2*Omega^3*alpha-2*Omega^5*xi2*alpha*mu
+4*Omega^5*epsilon*alpha*mu-xi2^2*omega^2*mu*Omega^3
-6*xi2*epsilon*mu*Omega^5+6*xi2*epsilon*Omega^3*alpha
-4*epsilon^2*omega^2*mu*Omega^3-omega2^2*omega^2*mu*Omega^3
```

```
-2*xi1*Omega^5*alpha*mu+4*xi1*Omega^5*xi2*mu-4*xi1*Omega^3*xi2*alpha
-6*xi1*Omega^5*epsilon*mu+6*xi1*Omega^3*epsilon*alpha
-8*xi1*xi2*epsilon*Omega^3-xi1^2*Omega^3*omega^2*mu
-2*xi1^2*Omega*xi2*omega^2+2*xi1^2*Omega*epsilon*omega^2
-xi1^2*xi2^2*mu*Omega^3+xi1^2*xi2^2*Omega*alpha
-xi1^2*epsilon^2*mu*Omega^3+xi1^2*epsilon^2*Omega*alpha
-xi1^2*omega2^2*mu*Omega^3+xi1^2*omega2^2*Omega*alpha
-epsilon^2*xi2^2*mu*Omega^3+epsilon^2*xi2^2*Omega*alpha
-epsilon^2*omega2^2*mu*Omega^3+epsilon^2*omega2^2*Omega*alpha
-4*Omega*xi2*epsilon^2*omega^2-2*Omega*xi1*xi2^2*omega^2
-4*Omega*xi1*epsilon^2*omega^2-2*Omega*xi1*omega2^2*omega^2
+2*Omega*epsilon*xi2^2*omega^2+2*Omega*epsilon*omega2^2*omega^2
-omega1^2*Omega^3*omega^2*mu-2*omega1^2*Omega*xi2*omega^2
+2*omega1^2*Omega*epsilon*omega^2-omega1^2*xi2^2*mu*Omega^3
+omega1^2*xi2^2*Omega*alpha-omega1^2*epsilon^2*mu*Omega^3
+omega1^2*epsilon^2*Omega*alpha-omega1^2*omega2^2*mu*Omega^3
+omega1^2*omega2^2*Omega*alpha+epsilon*Omega^3*k*cos(beta)
-Omega^7*mu+Omega^5*alpha-2*Omega^5*xi2+4*Omega^5*epsilon
-2*xi1*Omega^5+omega2^2*mu*Omega^5-omega2^2*Omega^3*alpha
+4*xi2*epsilon^2*Omega^3+2*xi1*xi2^2*Omega^3
-2*epsilon*xi2^2*Omega^3-2*epsilon*omega2^2*Omega^3
+xi1^2*Omega^5*mu-xi1^2*Omega^3*alpha+2*xi1^2*Omega^3*xi2
-2*xi1^2*Omega^3*epsilon+omega1^2*Omega^5*mu
+2*omega1^2*Omega^3*xi2-2*omega1^2*Omega^3*epsilon
+2*omega1^2*Omega^3*xi2*alpha*mu-2*omega1^2*Omega^3*epsilon*alpha*mu
+omega1^2*xi2^2*omega^2*mu*Omega+2*omega1^2*xi2*epsilon*mu*Omega^3
-2*omega1^2*xi2*epsilon*Omega*alpha
+omega1^2*epsilon^2*omega^2*mu*Omega+6*xi2*epsilon*omega^2*mu*Omega^3
+4*xi2*epsilon^2*alpha*mu*Omega^3-4*xi1*Omega^3*xi2*omega^2*mu
+6*xi1*Omega^3*epsilon*omega^2*mu+2*xi1*xi2^2*alpha*mu*Omega^3
+4*xi1*epsilon^2*alpha*mu*Omega^3+2*xi1*omega2^2*alpha*mu*Omega^3
-8*xi1*xi2*epsilon*alpha*mu*Omega^3-2*epsilon*xi2^2*alpha*mu*Omega^3
-2*epsilon*omega2^2*alpha*mu*Omega^3+2*xi1^2*Omega^3*xi2*alpha*mu
-2*xi1^2*Omega^3*epsilon*alpha*mu+xi1^2*xi2^2*omega^2*mu*Omega
+2*xi1^2*xi2*epsilon*mu*Omega^3-2*xi1^2*xi2*epsilon*Omega*alpha
+xi1^2*epsilon^2*omega^2*mu*Omega+xi1^2*omega2^2*omega^2*mu*Omega
-2*xi1^2*xi2*epsilon*omega^2*mu*Omega
+epsilon^2*xi2^2*omega^2*mu*Omega+epsilon^2*omega2^2*omega^2*mu*Omega
+8*Omega*xi1*xi2*epsilon*omega^2-2*xi1*xi2*epsilon^2*mu*Omega^3
+2*xi1*xi2*epsilon^2*Omega*alpha+2*xi1*epsilon*xi2^2*mu*Omega^3
```

```
-2*xi1*epsilon*xi2^2*Omega*alpha+2*xi1*epsilon*omega2^2*mu*Omega^3
-2*xi1*epsilon*omega2^2*Omega*alpha+2*xi1*xi2*epsilon^2*omega^2*mu*Omega
-2*xi1*epsilon*xi2^2*omega^2*mu*Omega
-2*xi1*epsilon*omega2^2*omega^2*mu*Omega
+omega1^2*omega2^2*omega^2*mu*Omega-2*omega1^2*xi2*epsilon*omega^2*mu*Omega
-2*omega1*epsilon^2*omega2*mu*Omega^3+2*omega1*epsilon^2*omega2*Omega*alpha
+2*omega1*epsilon^2*omega2*omega^2*mu*Omega
-epsilon*omega2*Omega^3*k*sin(beta)*mu+epsilon^2*omega2*Omega*k*sin(beta)
+epsilon^2*omega2*Omega*k*gm*sin(beta)+omega1*epsilon^2*Omega*k*sin(beta)
-xi1*epsilon*omega2*Omega*k*sin(beta)-xi1*epsilon*omega2*Omega*k*gm*sin(beta)
+omega1*epsilon*omega2*Omega*k*cos(beta)
+omega1*epsilon*omega2*Omega*gm*k*cos(beta)
+omega1*epsilon^2*Omega*k*gm*sin(beta)+2*epsilon^2*Omega^3*k*cos(beta)*mu
+xi1*epsilon^2*Omega*k*cos(beta)+xi1*epsilon^2*Omega*gm*k*cos(beta)
+epsilon^2*xi2*Omega*k*cos(beta)+epsilon^2*xi2*Omega*gm*k*cos(beta)
+epsilon*Omega^3*gm*k*cos(beta)-epsilon*omega1*Omega^3*k*sin(beta)*mu
-epsilon*omega1*xi2*Omega*k*sin(beta)-epsilon*omega1*xi2*Omega*k*gm*sin(beta)
-epsilon*xi2*Omega^3*k*cos(beta)*mu-epsilon*xi1*Omega^3*k*cos(beta)*mu
-epsilon*xi1*xi2*Omega*k*cos(beta)-epsilon*xi1*xi2*Omega*gm*k*cos(beta):
> gmk1:=solve(subs(gm=gmk/k,eqm), gmk):
> eqr1:=subs(gm=gmk1/k,eqr):
> k1:=solve(eqr1,k):
> gm1:=subs(k=k1,gmk1/k):
> omega1:=1.0; omega2:=1.0; omega:=1.0; alpha:=0.3*omega: beta:=0.; xi1:=0.02;
xi2:=0.02; mu:=500: epsilon:=0.05;

                              omega1 := 1.0


                              omega2 := 1.0


                               omega := 1.0


                                beta := 0.


                               xi1 := 0.02
```

```
                              xi2 := 0.02

                             epsilon := 0.05

> theta:=-arctan(gm1/omega/mu):
> plot([theta,k1*sqrt(1+gm1^2/omega^2/mu^2),Omega=0..2.0], -1.58..1.58,
-1...2,numpoints=500,thickness=2);
> N1:=1000;
> Omega1:=5./mu;
> N2:=5000;
> dtf:=array(1..N1+N2,1..3);
> for i from 1 to N1 do
> Omega:=evalf(Omega1/N1*i);
> dtf[i,1]:=Omega;
> dtf[i,2]:=evalf(theta);
> dtf[i,3]:=evalf(k1*sqrt(1+gm1^2/omega^2/mu^2));
> od:
> for i from N1+1 to N1+N2 do
> Omega:=evalf(Omega1+(5-Omega1)/N2*(i-N1));
> dtf[i,1]:=Omega;
> dtf[i,2]:=evalf(theta);
> dtf[i,3]:=evalf(k1*sqrt(1+gm1^2/omega^2/mu^2));
> od:

                              N1 := 1000

                         Omega1 := 0.01000000000

                              N2 := 5000

                  dtf := array(1 .. 6000, 1 .. 3, [])
> fd:=fopen( "E:\\work\\stability\\twoens\\ident.dat", WRITE ):
> writedata(fd,dtf):
> close(fd):
```

Bibliography

[1] J. C. Maxwell. On governors. In *Proc. Royal Soc. London*, volume 16, pages 270–283, London, 1868.

[2] I. A. Vishnegradsky. *On Controllers of Direct Action*. SPB Tekhnolog. Inst., St. Petersburg, 1877.

[3] B. van der Pol. *Phil. Mag.*, 3, 1927.

[4] E. V. Appleton. In *Proc. Cambrige Phil. Soc. (Math. and Phys. Sci)*, volume 21, pages 231–248, 1922.

[5] A. A. Andronov and A. G. Maier. O zadache Vyshnegradskogo v teorii pryamogo regulirovaniya. *Dokl. Akad. Nauk SSSR*, 47:345, 1945. (In Russian).

[6] A. A. Andronov and A. G. Maier. Zadacha Vyshnegradskogo v reorii pryamogo regulirovaniya. teoriya regulyatora pryamogo deystviya pri nalichii kulonovskogo i vyazkogo treniya. *Avtomatika i Telemechamika*, 8:314, 1947. (In Russian).

[7] A. A. Andronov and A. G. Maier. Zadacha Mizesa v teorii pryamogo regulirovaniya i teoriya tochechnyh preobrazovanii poverhnostey. *Dokl. Akad. Nauk SSSR*, 4(2):54–58, 1944. (In Russian).

[8] H. S. Black. Stabilized feedback amplifiers. *Bell Syst. Tech. J.*, 1934.

[9] R. E. Kalman. A new approach to linear filtering and prediction problems. *ASME J. Basic Eng.*, 82:34–45, 1960.

[10] A. A. Andronov and N. N. Bautin. Stabilizatsiya kursa neytralnogo samoleta avtopilotom s postoyannoy skorostyu servomotora i zonoy nechuvstvitelnosti. *Dokl. Akad. Nauk SSSR*, 46:158, 1945. (In Russian).

[11] O. Mayr. *Origins of Feedback Control*. MIT Press, Cambridge MA, 1970.

[12] J. Bechhoefer. Feedback for physicists: A tutorial essay on control. *Reviews of Modern Physics*, 77:783–836, 2005.

[13] K. Pyragas. Continuous control of chaos, by self-controlling feedback. *Phys. Lett. A*, 170:421–428, 1992.

[14] G. Franceschini, S. Bose, and E. Schöll. Control ofchaotic spatiotemporal spiking by time-delay autosynchronization. *Phys. Rev. E*, 60(5):5426–5434, 1999.

[15] W. Just, H. Benner, and E. Schöll. Control of chaos by time-delayed feedback: A survey of theoretical and experimental aspects. In B. Kramer, editor, *Advances in Solid State Physics*, volume 43, pages 589–603. Springer, Berlin, 2003.

[16] P. Parmananda and J. L. Hudson. Controlling spatiotemporal chemical chaos using delayed feedback. *Phys. Rev. E*, 64(3):037201, 2001.

[17] M. Bertram and A. S. Mikhailov. Pattern formation in a surface chemical reaction with global delayed feedback. *Phys. Rev. E*, 63(6):066102, 2001.

[18] D. Goldobin, M. Rosenblum, and A. Pikovsky. Controlling oscillator coherence by delayed feedback. *Phys. Rev. E*, 67(6):061119, 2003.

[19] D. Goldobin, M. Rosenblum, and A. Pikovsky. Coherence of noisy oscillators with delayed feedback. *Physica A*, 327(12):124128, 2003.

[20] A. H. Pawlik and A. Pikovsky. Control of oscillators coherence by multiple delayed feedback. *Phys. Lett. A*, 358(181-185):1, 2006.

[21] M. C. Mackey and L. Glass. Oscillation and chaos in physiological control systems. *Science*, 197:287–289, 1977.

[22] M. C. Mackey and L. Glass. *From Clock to Chaos: The Rhythms of Life*. Princeton Univ. Press, Princeton, NJ, 1988.

[23] P. S. Landa. *Self–Oscillations in Systems with Finite Number of Degrees of Freedom*. Nauka, Moscow, 1980. (In Russian).

[24] H. Daido and K. Nakanishi. Aging transition and universal scaling in oscillator networks. *Phys. Rev. Lett.*, 93:104101, 2004.

[25] D. Pazó and E. Montbrió. Universal behavior in populations composed of excitable and self-oscillatory elements. *Phys. Rev. E.*, 73:055202(R), 2006.

[26] P. A. Tass. *Phase Resetting in Medicine and Biology. Stochastic Modelling and Data Analysis.* Springer-Verlag, Berlin, 1999.

[27] G. Buzsáki and A. Draguhn. Neuronal oscillations in cortical networks. *Science*, 304:1926–1929, 2004.

[28] J. Milton and P. Jung, editors. *Epilepsy as a Dynamic Disease*. Springer, Berlin, 2003.

[29] S. A. Chkhenkeli. *Bull. of Georgian Academy of Sciences*, 90:406–411, 1978.

[30] S. A. Chkhenkeli. Direct deep brain stimulation: First steps towards the feedback control of seizures. In J. Milton and P. Jung, editors, *Epilepsy as a Dynamic Disease*, pages 249–261. Springer, Berlin, 2003.

[31] A.L. Benabid, P. Pollak, C. Gervason, D. Hoffmann, D.M. Gao, M. Hommel, J.E. Perret, and J. De Rougemont. Long-term suppression of tremor by chronic stimulation of the ventral intermediate thalamic nucleus. *Lancet*, 337:403–406, 1991.

[32] P. A. Tass, Ch. Hauptmann, and O. Popovych. Development of therapeutic brain stimulation techniques with methods from nonlinear dynamics and statistical physics. *Int. J. Bif. & Chaos*, 16(7):1889, 2006.

[33] O. Popovych, Ch. Hauptmann, and P. A. Tass. Effective desynchronization by nonlinear delayed feedback. *Phys. Rev. Lett.*, 94:164102, 2005.

[34] M. G. Rosenblum and A. S. Pikovsky. Controlling synchrony in ensemble of globally coupled oscillators. *Phys. Rev. Lett.*, 92:114102, 2004.

[35] M. G. Rosenblum and A. S. Pikovsky. Delayed feedback control of collective synchrony: An approach to suppression of pathological brain rhythms. *Phys. Rev. E.*, 70:041904, 2004.

[36] M. Rosenblum, L. Cimponeriu, N. Tukhlina, and A. Pikovsky. Delayed feedback suppression of collective rhythmic activity in a neuronal ensemble. *Int. J. Bif. & Chaos*, 16(7):1989–1999, 2006.

[37] N. Tukhlina, M. Rosenblum, A. Pikovsky, and J. Kurths. Feedback suppression of neural synchrony by vanishing stimulation. *Phys. Rev. E*, 75:011019, 2007.

[38] J. E. Rubin and D. Terman. High frequency stimulation of the subtalamic nucleus eliminates pathological thalamic rhythmicity in a computational model. *J. Comp. Neurosci.*, 16:211–235, 2004.

[39] M. C, J. A. Obeso, A. E. Lang, P. Pollak J. L Houeto, and S. Rehncrona et al. Bilateral deep brain stimulation in parkinsons disease: a multicentre study with 4 years follow-up. *Brain*, 128:2240–9, 2005.

[40] S. H. Strogatz, D. M. Abrams, A. McRobie, B. Eckhardt, and E. Ott. Theoretical mechanics: Crowd synchrony on the Millennium Bridge. *Nature*, 438:43–44, 2005.

[41] P. Dallard, T. Fitzpatrick, A. Flint, A. Low, R. Ridsill Smith, M. Willford, and M. Roche. London millennium bridge: Pedestrian-induced lateral vibration. *J. Bridge Eng.*, 6:412–417, 2001.

[42] J. Hudson, private comminucation.

[43] H. Bergman, A. Feingold, A. Nini, A. Raz, H. Slovin, M. Abeles, and E. Vaadia. Physiological aspects of information processing in the basal ganglia of normal and parkinsonian primates. *Trends Neurosci.*, 21:32, 1998.

[44] J. Sarnthein, A. Morel, A. von Stein, and D. Jeanmonod. Thalamic theta field potentials and EEG: High thalamocortical coherence in patients with neurogenic pain, epilepsy and movement disorders. *Thalamus & Related Systems*, 2:321, 2003.

[45] J. A. Goldberg, U. Rokni, T. Boraud, E. Vaadia, and H. Bergman. Spike synchronization in the cortex-basal ganglia network of parkinsonian primates reflects global dynamics of the local field potentials. *J. Neurosci.*, 24:6003, 2004.

[46] M. Magnin, A. Morel, and D. Jeanmonod. Single-unit analysis of the pallidum, thalamus and subtalamic nucleus in parkinsonian patients. *Neuroscience*, 96(3):549, 2000.

[47] Y. Kuramoto. *Chemical Oscillations, Waves and Turbulence*. Springer, Berlin, 1984.

[48] J. A. Acebron, L. L. Bonilla, C. J. Perez Vicente, F. Ritort, and R. Spigler. The kuramoto model: A simple paradigm for synchronization phenomena. *Reviews of Modern Physics*, 77(1):137–175, 2005.

[49] K. Pyragas, V. Pyragas, I.Z. Kiss, , and J. L. Hudson. Adaptive control of unknown unstable steady states of dynamical systems. *Phys. Rev. E.*, 92:026215, 2004.

[50] D. V. R. Reddy, A. Sen, and G. L. Johnston. Dynamics of a limit cycle oscillator under time delayed linear and nonlinear feedbacks. *Physica D*, 144(3-4):335–357, 2000.

[51] F. M. Atay. Delayed-feedback control of oscillations in non-linear planar systems. *Int. J. Control*, 75:297–304, 2002.

[52] F. M. Atay. Oscillation control in delayed feedback systems. In *Dynamics, Bifurcation, and Control*, volume 273 of *Lecture Notes in Control and Information Sciences*, pages 103–116. Springer-Verlag, Berlin, 2002.

[53] P. Hövel and E. Schöll. Control of unstable steady states by time-delayed feedback methods. *Phys. Rev. E.*, 72:046203, 2005.

[54] M. A. Hassouneh, H.-C. Lee, and E. H. Abed. Washout filters in feedback control: Benefits, limitation and extensions. In *Proceeding of the 2004 American Control Conference*, pages 3950–3955. AACC, Boston, MA, 2004.

[55] M. A. Hassouneh, H.-C. Lee, and E. H. Abed. Washout filters in feedback control: Benefits, limitations and extensions. Technical report, Institute for Systems Research, 2004.

[56] N. F. Rulkov. Regularization of synchronized chaotic bursts. *Phys. Rev. Lett.*, 86(1):183–186, 2001.

[57] U. Mitzdorf. Current source-density method and application in cat cerebral cortex: investigation of evoked potentials and eeg phenomena. *Physiological Reviews*, 65(1):37–90, 1985.

[58] Peter beim Graben. *Symbolische Dynamik ereigniskorrelierter Gehirnpotentiale in der Sprachverarbeitung.* PhD thesis, Universität Potsdam, 2000.

[59] J. L. Hindmarsh and R. M. Rose. A model for neuronal bursting using three coupled first order differential equations. *Proc. Roy. Soc. London Ser. B*, 221:87, 1984.

[60] R. Huerta, M. I. Rabinovich, H. D. I. Abarbanel, and M. Bazhenov. Spike-train bifurcation scaling in two coupled chaotic neurons. *Phys. Rev. E*, 55(3):R2108–R21010, 1997.

[61] L. Cimponeriu, M.G. Rosenblum, T. Fieseler, J. Dammers, M. Schiek, M. Majtanik, P. Morosan, A. Bezerianos, and P. A. Tass. Inferring asymmetric relations between interacting neuronal oscillators. *Progress of Theoretical Physics Suppl.*, 150:22–36, 2003.

[62] E. Montbrio, J. Kurths, and B. Blasius. Synchronization of two interacting populations of oscillators. *Phys. Rev. E.*, 70:056125, 2004.

[63] K. Pyragas, O. V. Popovych, and P. A. Tass. Controlling synchrony in oscillatory networks with a separate stimulation-registration setup. *EPL*, 80:40002, 2007.

[64] A. Pikovsky, M. Rosenblum, and J. Kurths. *Synchronization. A Universal Concept in Nonlinear Sciences*. Cambridge University Press, Cambridge, 2001.

[65] N.N Bogoliubov and Y.A Mitropolsky. *Asymptotic Methods in the Theory of Nonlinear Oscillations*. Gordon and Breach, New York, 1961.

[66] N. B. Janson, A. G. Balanov, and E. Schöll. Delayed feedback as a means of control of noise-induced motion. *Phys. Rev. Lett.*, 93:010601, 2004.

Acknowledgments

I would like to thank all the people who helped me in every way to make this work possible. First, I want to express my deepest gratitude to Prof. Dr. Kurths for offering me the opportunity to work in his group and for all his support, advisement and his valuable guidance during all these years.

I am profoundly grateful to Dr. Michael Rosenblum for his immense help, patience, endless stimuli and discussions. His ideas and tremendous support (not only in scientific matters) had a major influence on this thesis. I learned a lot during this time and I am convinced that this knowledge will help me in the future.

My special thanks are addressed to Prof. Dr. Arkady Pikovsky for interesting discussions, fruitful collaborations and helpful advice on my works. I have been privileged to benefit from his comprehensive expertise.

My warmest thanks go to Prof. Polina Landa, who was a supervisor of my diploma work during my studies at the Moscow State University, for her guiding and encouraging me. With her vast knowledge, enthusiasm, and manner of scientific thinking, she has given me an admirable role-model as a researcher.

I sincerely thank Denis Goldobin for his kind help, fruitful scientific advice, discussions and for proof-readings of this manuscript.

My thanks to my friends and colleagues for the great time I had in our group. Especially to Priya, Aneta, Young, Artur, Stefan, Arghya. I enjoyed the atmosphere, your friendship and your support. Thank you! I specially thank my closest friends Lucia and Kristina for helping me to keep myself in one piece in the changeable periods of this studies.

My thanks to the people from AGNLD and Helmholtz Center for Mind and Brain Dynamics, for the warm atmosphere of the meetings and fruitful discus-

sions.

My thanks to Birgit Voigt for help on administrative matters and Jörg Tessmer for help on technical problems.

My warmest thanks go to my mother and father for their love, support and for always encouraging me in everything I decide to do. Special thanks to my sister Marina for her help and revising the language of this thesis. And of course, I warmly thank Steve for his love, moral support and for keeping faith in me.

The acknowledgment list would be not complete without N. Brilliantov, L. Cimponeriu, A. Balanov, N. Janson.